2D SEISMIC DATA INTERPRETATION AND PETROPHYSICAL ANALYSIS OF MIANO GAS FIELD, LOWER INDUS BASIN, PAKISTAN

By

MUHAIMAN GUL (01-166222-010)

YAMEENA EMAN (01-166222-018)

DEPARTMENT OF EARTH AND ENVIRONMENTAL SCIENCES

BAHRIA UNIVERSITY, ISLAMABAD

2026

2D SEISMIC DATA INTERPRETATION AND PETROPHYSICAL ANALYSIS OF MIANO GAS FIELD, LOWER INDUS BASIN, PAKISTAN

A thesis submitted to Bahria university, Islamabad in partial fulfillment of the requirements for the degree of BS in Geophysics

By

MUHAIMAN GUL (01-166222-010)

YAMEENA EMAN (01-166222-018)

DEPARTMENT OF EARTH AND ENVIRONMENTAL SCIENCES

BAHRIA UNIVERSITY, ISLAMABAD

2026

ABSTRACT

The thesis used 2D seismic interpretation to observe and comprehend the subsurface geology of the Miano region, and petrophysical formulas were used to estimate the hydrocarbon saturation. The studied region is impacted by extensional tectonics, which results in normal faults that are visible in interpreted seismic sections. Because of the trend of these faults, the area contains graben and horst structures that aid in the accumulation of hydrocarbons. The Upper Goru serves as a seal, completing the petroleum system, whereas the Lower Goru is the reservoir formation and the Sembar Formation is the main source rock in the research region. This thesis created time and depth contour maps of the Lower Goru and Ranikot formations after marking three horizons on a seismic section known as Lower Goru of the Cretaceous age, Sui Main Limestone of the Eocene age. The Lower Goru Formation was subjected to petrophysical study, and four hydrocarbon-bearing zones were found based on the log curve. Average shale volume, hydrocarbon saturation, and effective porosity values were computed for these zones.

ACKNOWLEDGEMENT

We want to sincerely thank our family for their continuous support. Their selflessness and unwavering inspiration were essential to our group's success. We also want to express our sincere gratitude to our supervisor, Dr. Urooj Shakir, for their tremendous patience, priceless wisdom, and guidance that have greatly aided us in our progress. We are also very appreciative of all the collaborations and assistance that our classmates have given us. We also owe a debt of gratitude to doctorate scholar Haris for his tremendously helpful support. Lastly, we would like to sincerely thank everyone else who has helped us over the past year.

TABLE OF CONTENTS

List of Figures

LIST OF TABLES

CHAPTER 1

INTRODUCTION

1.1 Techniques

The seismic reflection technique is one of the most popular and dependable geophysical methods for subsurface investigation, notably in petroleum exploration. Its significance stems from its capacity to provide precise images of underground geological features at depths that are often beyond the reach of many other geophysical methods. Because hydrocarbons like oil and gas are often contained in deeply buried sedimentary formations, seismic reflection has become an important technique for detecting and evaluating possible reservoirs.

This method is non-intrusive, producing seismic waves with a source such as a vibroseis vehicle that enters the ground, impacting and reflecting off each subsurface layer. These waves are then recorded using geophones (Sheriff and Geldart, 1995).

The seismic reflection technique has a significant advantage over other geophysical approaches in terms of resolution. While gravity and magnetic surveys are important for regional information about subsurface conditions, they do not typically produce the same amount of structural detail. Seismic reflection, on the other hand, can clearly indicate the depth and geometry of subsurface formations. This makes it particularly effective in sedimentary basins, where tiny structural and stratigraphic differences might influence hydrocarbon occurrence.

In contrast, Petrophysics is also an important technique in the world of hydrocarbon exploration and production. Petrophysical analysis evaluates rock properties and their interaction with fluids utilizing data from well logs, core samples, and seismic surveys (Tiab & Donaldson, 2024).

Petrophysics technique involves interpreting well log data (such as gamma ray, resistivity, density, and neutron logs) as well as core samples in order to estimate critical reservoir parameters such as porosity, permeability, water saturation, and lithology. These features are critical for determining a reservoir's quality and productivity, as well as predicting how much oil or gas it may contain. While seismic reflection aids in detecting possible reservoirs, petrophysics offers precise information on whether those reservoirs are economically viable.

1.2 Study Area

The Miano Field is situated in the Central Indus Basin, approximately 62 kilometers southeast of Sukkur City in Khairpur district, Sindh province, Pakistan. The field is 814 km² and is located in the Thar Desert region. The Miano gas field is located between the latitudes of **27°37'55.3"N** and **27°37'18.98"N** and the longitudes of **69°31'26.36"E** and **69°31'59.73"E**. It is one of Pakistan's greatest natural gas producing fields in the southwest Indus Basin.

The study region is located on the Panno-Aqil graben, which is surrounded by structural highs like Mari-Kandhkot and Jacobabad-Khairpur. It is part of an extensional regime in the Indus Basin that is distinguished by normal faulting and horst-graben formations.

The Lower Goru is a significant reservoir that has produced hydrocarbons over the past two decades. We investigate the Goru reservoir through preliminary seismic interpretation utilizing 2D seismic profiles from the Miano gas field in Pakistan.

The Miano gas field has been the site of roughly 34 drilled wells (up to 2020), providing extensive subsurface data such as well logs and core samples for reservoir assessment.

The area is mostly composed of sedimentary rocks spanning in age from Permian to Mesozoic, with the Lower Goru Formation (Cretaceous) serving as the primary hydrocarbon reservoir. The region has tremendous petroleum potential due to the presence of structural and stratigraphic traps, and it has been a major gas producer since its discovery in 1993.

The Central Indus Basin is a large hydrocarbon-producing basin in Pakistan, located between major tectonic features such as the Thrust Belts, Indian Basement, and Kirthar Fold Belt. The basin is distinguished by extensional tectonics and passive roof complex structures, which are visible in seismic data. These structural features form an important geological framework for hydrocarbon formation. The tectonic setting of the research area is critical for understanding the subsurface layout and reservoir distribution within the basin.

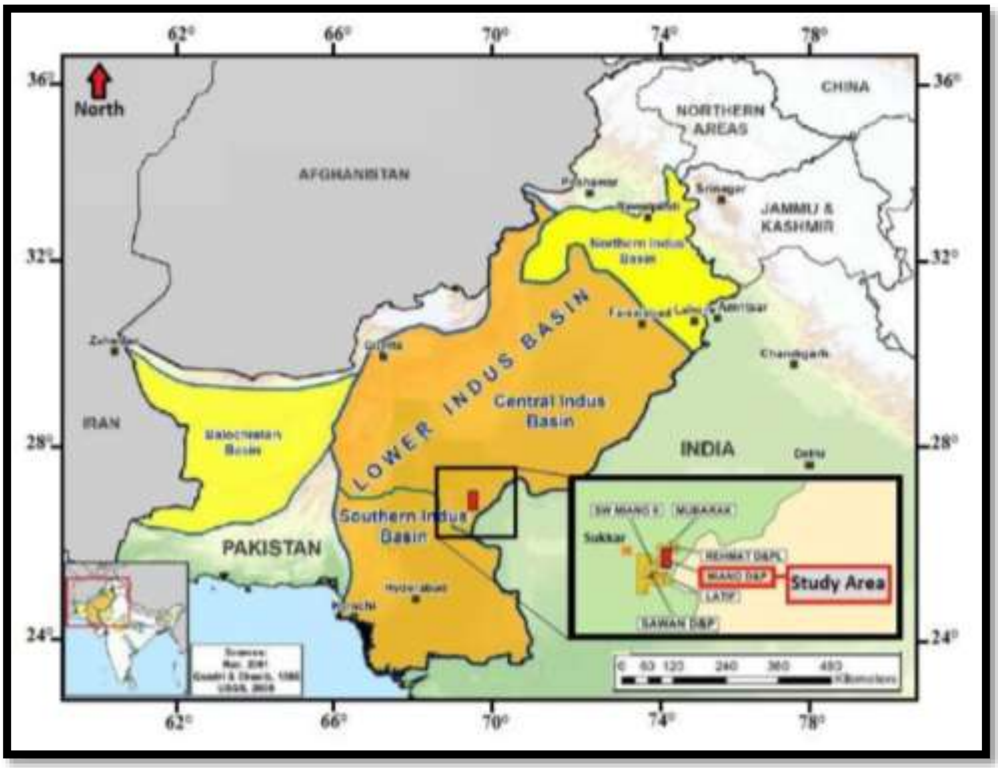

Figure 1.1 View of the study area of Central Indus Basin showing the location of Miano area (Courtesy by OMV)

1.3 Accessibility and Climate

Miano lies in the Sukkur district and is a flat location with lush flora. Several highways link to the district Sukkur, eventually leading to the Miano field region (Awan et al., 1999).

The study area's climate is hot and foggy during the summer, but dry and chilly during the winter. During January, the temperature ranges from 7 to 22°C (45 to 72°F), whereas the summer season begins in March-April and ends before October. Before the monsoon, the average temperature in June is 35°C (95°F), but it can reach 42°C (108°F). The average rainfall in this region is 88mm, with a range of 0.59 mm to 25.62 mm each month

1.4 Exploration History

The Miano area's exploration history is strongly tied to the larger hydrocarbon exploration activity in Pakistan's lower Indus Basin. The Miano Gas Field was discovered in 1993 after 2D seismic data analysis revealed interesting underlying features. The region received great attention due to its excellent tectonic location and demonstrated petroleum potential.

The first appraisal well, Miano-02, located 9 km north-northeast of the discovery well, was drilled in August 1994 and reached a total depth of 3553.5 m KB in the Lower Goru "upper shale". The "Massive sand" had the same thickness as Miano-01 but a much higher rate.

The second appraisal well, Miano-03, was spudded on December 21, 1994, 9 kilometers southwest of Miano-02. It has reached a total depth of 3466.5 m KB in the Lower Goru "Upper Shale" interval. The "Massive sand" interval proved to be tight, with no flow recorded during the test, and the third is the Miano-05, which was a development well with a total depth of 3400 m KB in the Lower Goru Formation.

Regional research in the Indus Basin began in the mid-twentieth century with geological mapping and surface studies, followed by gravity, magnetic, and seismic surveys.

With advances in seismic technology in the late twentieth century, more thorough subsurface imaging was performed in the Central Indus Basin, resulting in the identification of numerous structural and stratigraphic traps.

Approximately 34 wells have been drilled in the Miano field (until 2020). Following the discovery of gas in the Lower Goru Formation, further development and exploratory drilling occurred.

By 2020, around 34 wells had been drilled, which included both exploration wells and development/production wells. Only a few of these wells are active and producing gas, while the others have been completed or suspended.

1.5 Objectives

The study's goal is to gain a better understanding of the reservoir characteristics of wells using petrophysical techniques by evaluating their logs, which includes subsurface interpretation through the marking of horizons and faults to pinpoint the structure as well as hydrocarbon potential evaluation based on petrophysical analysis of the wells.

1.7 Data And Software

The data below was gathered with the consent of the Director General of Petroleum Concessions (DGPC), Petroleum House.

The dataset contains:

- **i.** Navigation files.
- **ii.** Seismic lines (SEGYS)
- **iii.** Seismic velocity headers
- **iv.** Well topped.
- **v.** Well headers.
- **vi.** Well logs (Digital Las files)

The software includes:

- **i.** Use Kingdom software for 2D seismic interpretation.
- **ii.** Use Gverse program for petrophysical analysis.

Table 1.1 Dataset (Seismic and Well)

<table>
<tr><th colspan="3">Seismic</th><th colspan="2">Well</th></tr>
<tr><th>Lines</th><th>Line Types</th><th>Orientation</th><th>Well Names</th><th>Logs</th></tr>
<tr><td>OMV/P2092-110</td><td>Inclined Line</td><td>SW To NE</td><td rowspan="3">MIANO- 02</td><td rowspan="6">Gamma ray
Spontaneous
Potential logs
Caliper logs
Density logs
Neutron Log
Resistivity Log
Sonic Log
PEF</td></tr>
<tr><td>OMV/P2092-111</td><td>Dip Line</td><td>WE</td></tr>
<tr><td>OMV/P2092-113</td><td>Dip Line</td><td>WE</td></tr>
<tr><td>OMV/P2092-114</td><td>Strike Line</td><td>NS</td><td rowspan="3">MIANO- 03</td></tr>
<tr><td>OMV/P2092-115</td><td>Dip Line</td><td>WE</td></tr>
<tr><td>OMV/P2092-117</td><td>Dip Line</td><td>WE</td></tr>
</table>

1.8 Methodology

Figure 1.2 illustrates the methods used with two workflows: seismic and petrophysics. The seismic data is loaded into Kingdom software, and all subsequent operations are likewise performed with Kingdom software, whilst the well data is processed using Petrol software until hydrocarbon saturation is computed. The findings from both procedures are combined for final conclusion and interpretation.

Accurate reservoir characterization relies heavily on an integrated workflow of seismic interpretation and petrophysical analysis. The seismic procedure starts with creating a project in interpretation software like Petrol, then loads navigation data and imports seismic data in SEG-Y format. A basemap is created to display the geographic distribution of seismic lines, and detailed interpretation is performed by selecting horizons and detecting faults. These interpreted horizons are then transformed from time to depth using velocity data, allowing structural grids and contour maps to be generated, which specify the reservoir's geometry and trapping configuration. Seismic migration is used to correct reflector placements and provide an accurate view of the subsurface.

In parallel, the petrophysical workflow evaluates reservoir parameters by analyzing well log data such as gamma ray, resistivity, density, and neutron logs. These logs are used to determine critical metrics such as shale volume, porosity, and water saturation. The hydrocarbon saturation is then calculated, providing information about the reservoir's fluid content. The integration of these two techniques creates a full reservoir model by combining structural information from seismic data with rock and fluid parameters from petrophysical analysis. This integrated strategy allows for the identification of hydrocarbon-bearing zones, the estimate of reserves, and the optimization of drilling locations, resulting in more dependable exploration and production decisions.

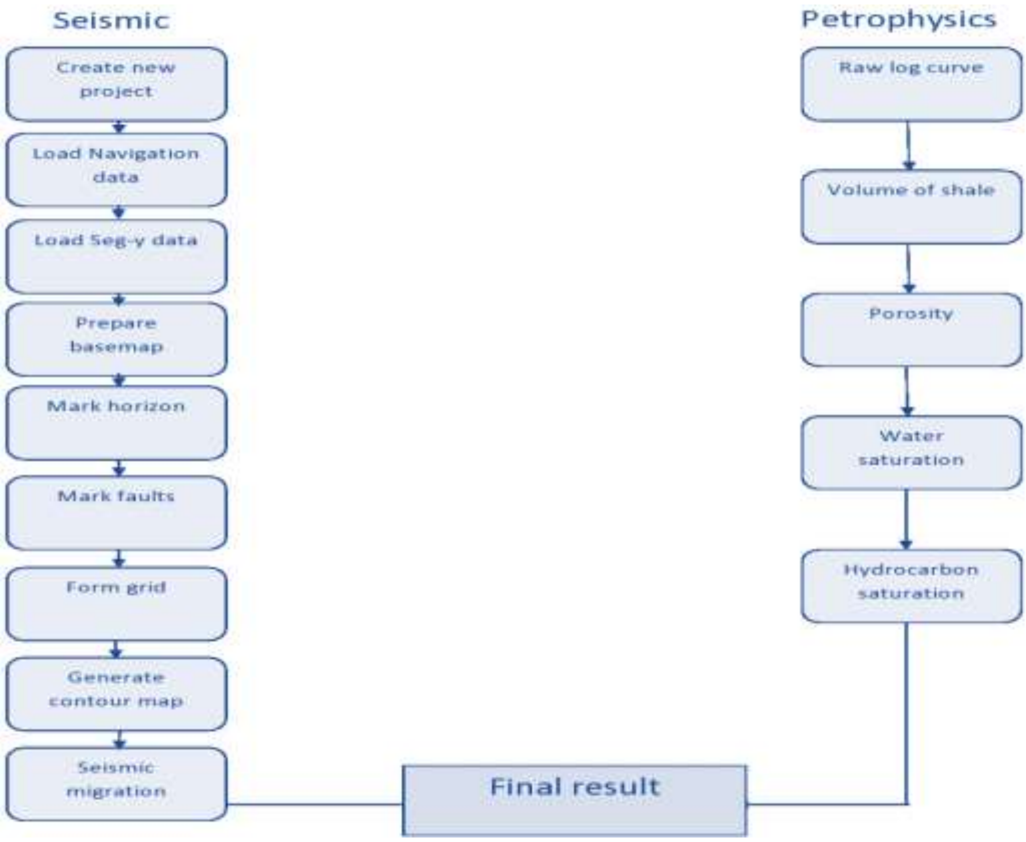

Figure 1.2 depicts the full process involving seismic and petrophysics.

CHAPTER 2
TECTONICS AND GENERAL GEOLOGY

2.1 Regional Tectonics

The tectonics of the Lower Indus Platform Basin trace the Indian Plate's passage from a Gondwanan rift fragment to its dramatic collision with the Eurasian Plate. The basin's architecture is principally determined by three major tectonic phases: Mesozoic extensional rifting, Late Cretaceous thermal perturbation, and Cenozoic compressive inversion. The Lower Indus Platform Basin's tectonic framework is defined by a complex evolutionary history that saw it go from a passive edge rift system to a concentrated zone of collisional deformation. The Indian Plate rifted from Gondwanaland during the Jurassic to Early Cretaceous Period, establishing the foundational tectonic architecture. This extensional phase triggered N-S to NE-SW trending normal faults, resulting in a characteristic horst-and-graben geometry across the platform.

These tilted fault blocks are crucial to the region's geology, serving as major structural containers for sediment buildup and later hydrocarbon localization. During this time, the basin served as a passive border, gradually subsiding and allowing the deposition of thick Mesozoic clastic and carbonate layers.

By the Late Cretaceous, the tectonic regime had evolved substantially when India separated from Madagascar and the plate interacted with the Reunion hotspot. This epoch was marked by substantial thermal doming and isostatic uplift, which caused widespread erosion and the creation of the well-known Base Tertiary Unconformity. The extrusion of the Deccan flood basalts, which brought a heat pulse into the basin's history, had an additional impact on the related strike-slip faulting and NNW-striking normal faults. This fragmentation phase fundamentally altered the earlier rift architecture, producing new fracture networks and changing the regional stress field prior to the commencement of substantial plate convergence.

The shift into the Cenozoic period brought the northward-moving Indian Plate into close contact with the Afghan Block and the Eurasian Plate, dramatically altering the basin's western and northern limits. The Bela Ophiolites were deposited and gently folded during the Paleocene and Eocene, but most of the Eocene was distinguished by structural quiescence and the formation of carbonate platforms. However, from the Oligocene to the present, the continuous Himalayan collision has exposed the basin to severe sinistral transpression. This compressive force has overprinted the ancient rift structures with fold-thrust belts and elaborate "flower structures" along the western edge.

Currently, the Lower Indus Platform Basin is a dynamic tectonic province within the Indus Foredeep. The combination of stable basement highs, such as the Jacobabad-Khairpur and Mari-Kandhkot Highs, with mobile fold belts of the Sulaiman and Kirthar ranges dominates the structural landscape. While the eastern platform retains the original extensional rifting and passive margin sedimentation, the western and northwestern sections show the consequences of crustal shortening, with thrust-faulted anticlines and inverted structures formed by the severe tectonic collision. This multiphase history, which ranges from extensional rifting and thermal doming to collisional transpression, continues to shape the basin's complex structural geometry and sedimentary distribution.

2.2 Tectonic Framework

The Lower Indus Platform Basin is a complex structural mosaic that acts as a transition zone between the stable Indian Shield and the dynamic collisional limits to the west. Geographically, the basin is surrounded to the north by the Central Indus Basin, northwest by the Sulaiman Fold Belt, and southwest by the Kirthar Fold Belt. The location is located in the "IndusPlatform and Foredeep" tectonic province, which is defined by a foundational structural architecture formed during the Mesozoic rifting of the Indian Plate from Gondwanaland. This extensional phase kicked off a succession of NE-SW to N-S trendingrift systems, resulting in a characteristic horst-and-graben geometry across the platform. These tilted fault blocks are crucial to the region's geology, serving as key structural containers for sediment accumulation and establishing the targets for current seismic interpretation.

The structural landscape is dominated by the interaction of stable basement structures, such as the Jacobabad-Khairpur and Mari-Kandhkot Highs, with mobile fold belts in the west. While the eastern platform represents a history of passive margin sedimentation, the western and northwestern parts show the severe consequences of crustal shortening. The severe tectonic collision between the Indian and Eurasian plates resulted in characteristics such as thrust-faulted anticlines and inverted structures.

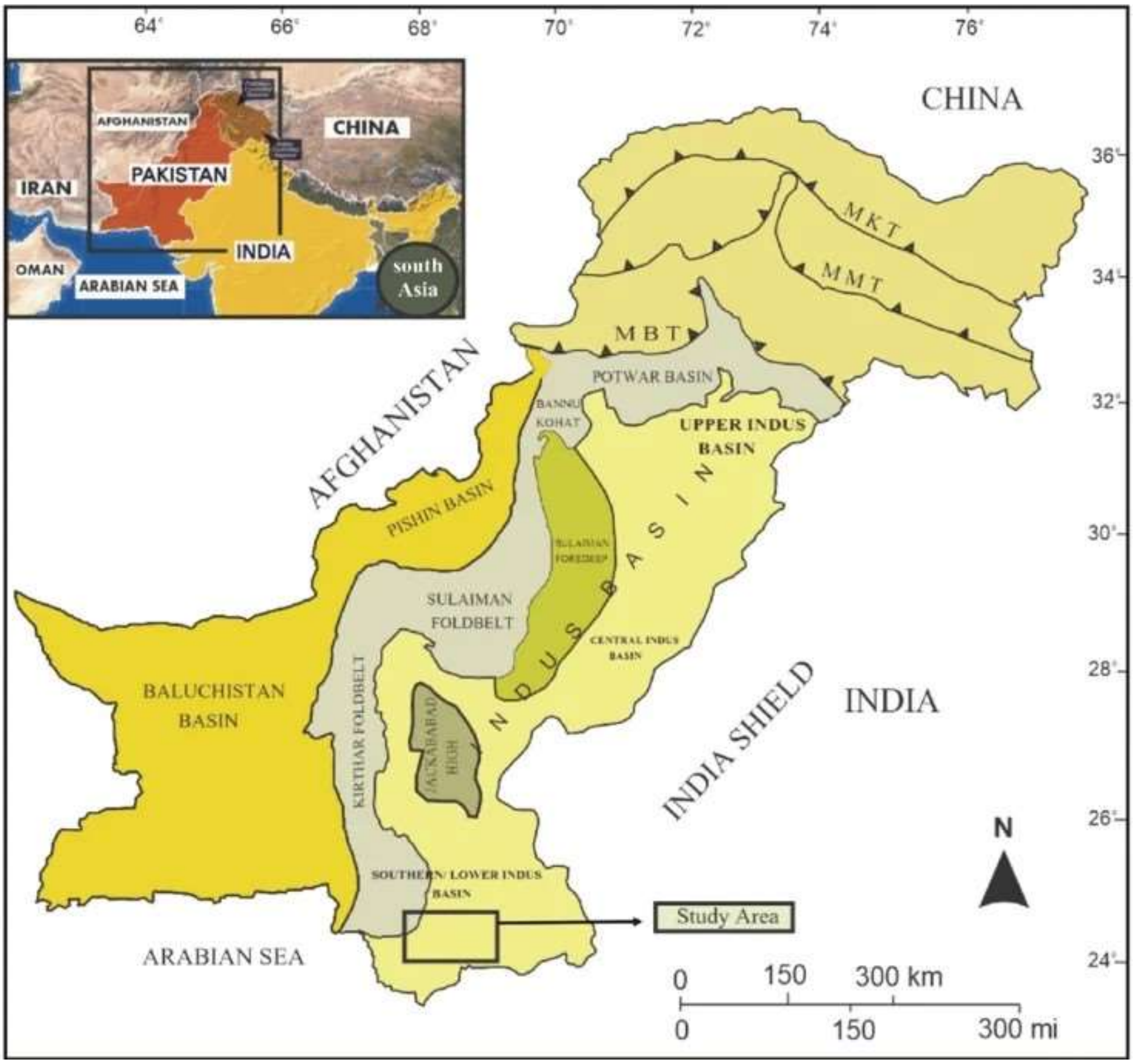

Figure 2.1 Tectonic map of Pakistan showing sedimentary basins.(after Kazmi & Jan1997).

Along the western edge, old rift structures have frequently been overprinted by sinistral transpression, resulting in intricate "flower structures" apparent on 2D seismic profiles. This tectonic province is supported by an infra-Cambrian to Recent sequence of clastics and carbonates, with a Precambrian basement that deepens dramatically to the west.

By the Late Cretaceous, the tectonic regime had transformed when India separated from Madagascar and the plate interacted with the Reunion hotspot. Thermal doming, strike-slip faulting, and the extrusion of Deccan flood basalts all occurred during this time period, resulting in notable NNW-striking normal faults and extensive thermal pulses. These episodes caused extensive uplift and erosion, resulting in the conspicuous Base Tertiary Unconformity, a major seismic reflector throughout the basin. In the eastern section of the basin, this erosional event is so significant that the Tertiary sequence frequently comes into direct touch with the Jurassic strata.

The emplacement of the Bela Ophiolites and subsequent gentle folding added to the intricacy of the Cenozoic transition, finally leading to the contemporary foredeep setting. This multiphase history, which ranges from extensional rifting and thermal doming to collisional transpression, continues to shape the basin's complex structural geometry and the petrophysical properties of its sedimentary fill.

2.3 General Geology and Tectonics

The study area is part of the central Indus basin that has been identified as an extensional basin resulting from an inferred fossil rift crustal feature and is overlain by a thick sedimentary sequence. It is characterized by horst and graben structures, together with a system of transcurrent faults. The sands in Goru are of great importance and are widely distributed from Waziristan to as far south as Cutch in India. Regionally considering the Goru sediments their thickness increases towards the center of Karachi Embayment. The Goru Formation is dominantly shale or mudstone, mainly calcareous. The Lower Goru has been applied to the lower sandy member whereas the shale unit is preferred as Upper Goru Formation.

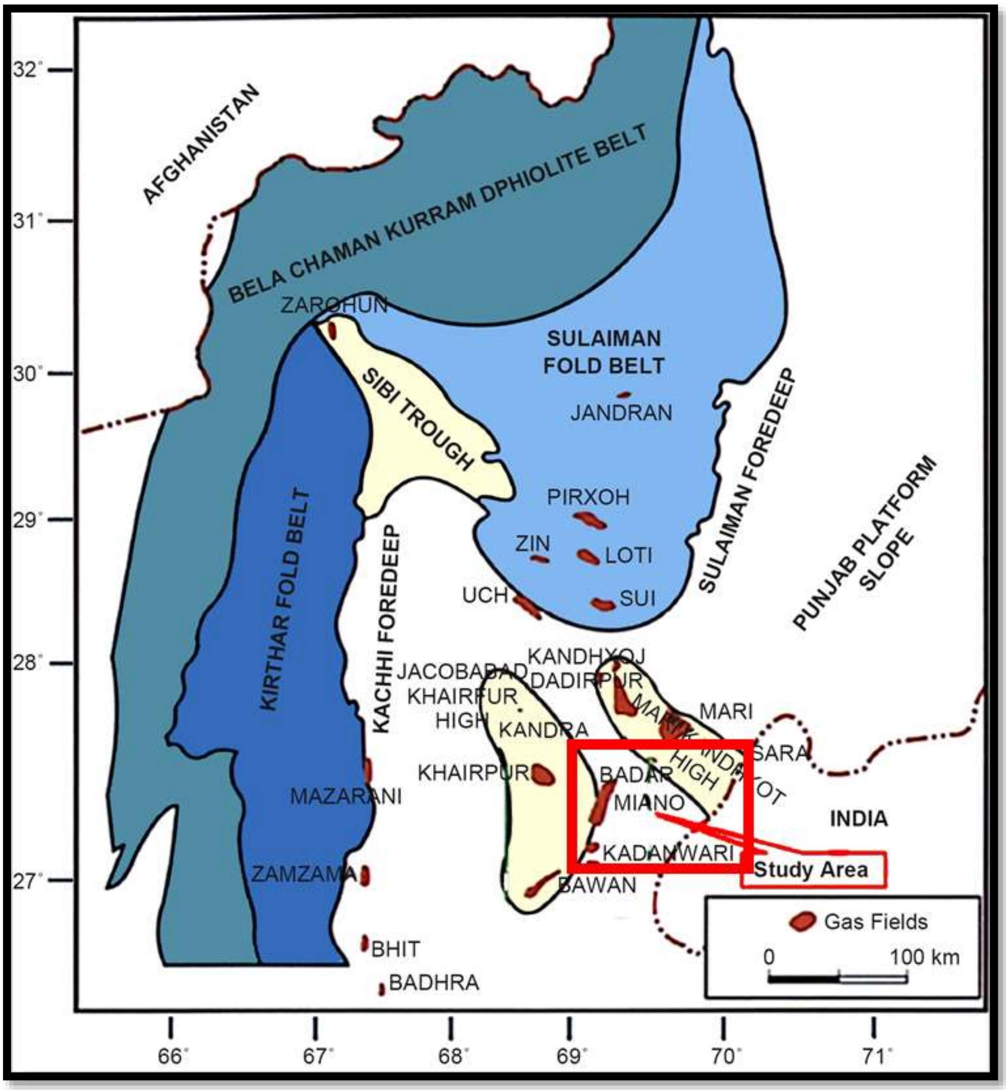

Figure 2.2 Tectonic map of Central Indus Basin showing the location of Miano block in Pano Aqill Graben. (Saif et al., 2016).

2.4 Generalized stratigraphy

The Indus Basin of Pakistan is the country's largest onshore sedimentary province, comprising approximately 138,000 square kilometers. According to Shakeel (2014), The Lower Indus Basin's stratigraphic architecture is strongly influenced by the Early Cretaceous succession, which demonstrates great lithological variation throughout the basin. This variation is mostly due to oscillations in sediment supply and shifting paleoenvironmental conditions during the Mesozoic. According to (Kadri 1995; Khalid et al. 2012; Shakeel 2014), The Goru Formation is at the heart of this succession, and it is lithologically divided into two different units: the Upper Goru and the Lower Goru. The Upper Goru is mostly made up of thick shale layers with minimal sandstone intercalations, but the Lower Goru is distinguished by a sand-dominant lithology that serves as the principal focus of petroleum exploration.

The Lower Goru Formation is classified chronologically as Barremian to Cenomanian, with occasional extensions into the Early Turonian period. These sandstone units are of great economic importance because of their confirmed hydrocarbon potential and complicated reservoir geometries. The quality and continuity of these reservoirs are influenced by a complex interaction of depositional settings, provenance, diagenesis, and the tectonic history of the Indian Plate's passive border. Within this paradigm, sequence stratigraphy offers the crucial background for comprehending cyclic sedimentation trends. The spatial and temporal distribution of reservoir bodies can be determined by examining relative sea-level fluctuations and third-order system tracts, especially in lowstand system tracts where sand buildup is most evident (Ahmed et al.,2014).

The basin's stratigraphic complexity frequently requires the discovery of subtle non-structural and combination traps. These trapping methods rely heavily on the lateral distribution and volume of clastic reservoirs, which might be unpredictable due to facies fluctuations. Major unconformities in the eastern section of the basin, particularly at the Permian and Tertiary base, complicate the stratigraphic record by bringing the Tertiary sequence into direct contact with Jurassic layers. As a result, the combination of net sand isopach mapping and sequence stratigraphic analysis is critical for identifying reservoir geometries and estimating the distribution of high-quality sands within the Lower Goru's overall shaly matrix. This stratigraphic framework serves as the foundation for future petrophysical evaluation and seismic interpretation.

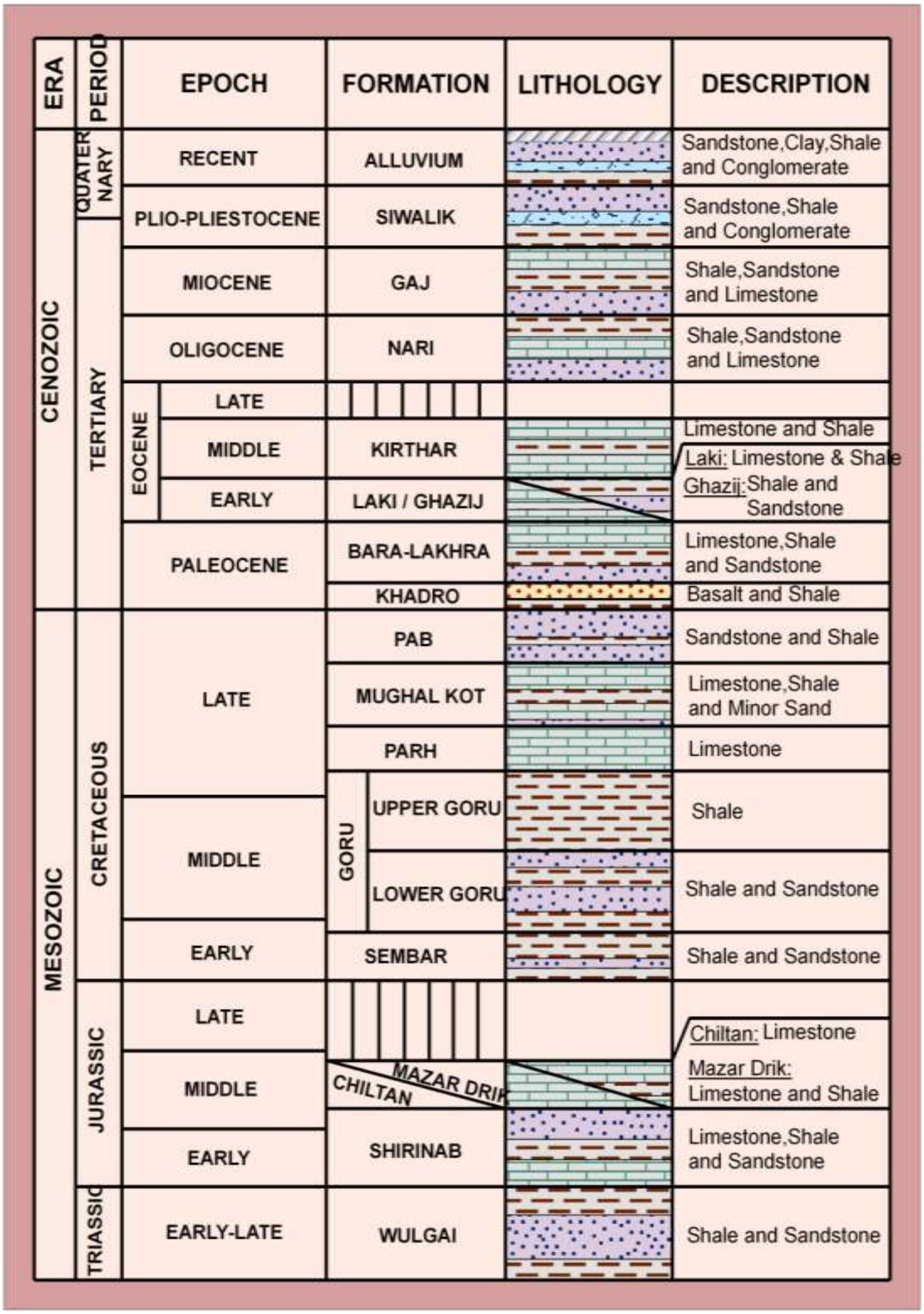

Figure 2.3. General stratigraphy of Middle Indus Basin Pakistan (Raza et al., 1990).

2.5 Borehole stratigraphy

Following stratigraphic tops are included in the Miano-02 well

Table 1.2 Borehole stratigraphy of Miano 02

BOREHOLE STRATIGRAPHY OF MIANO-02			
Formation	**Age**	**Tops**	**Thickness (m)**
Siwalik	Miocene-Pleistocene- Pliocene	0.00	500.00
Drazinda	Eocene	500.00	67.00
Pirkoh	Eocene	567.00	104.00
Sirki	Eocene	671.00	69.00
Habib Rahi	Eocene	740.00	124.00
Ghazij Member	Eocene	864.00	619.00
Sui Main Limestone	Eocene	1483.00	193.00
Ranikot	Paleocene	1676.00	123.00
Parh Limestone	Late Cretaceous/Early Cretaceous	1799.00	100.00
Upper Goru	Late Cretaceous/Early Cretaceous	1899.00	327.00
Lower Goru	Early Cretaceous	2226.00	1322.00

Table 1.3 Borehole stratigraphy of Miano 03

BORE HOLE STRATIGRAPHY OF MIANO-03			
Formation	**Age**	**Tops**	**Thickness(m)**
Siwalik	Miocene-Peistocene-Pliocene	0.00	269.00
Drazinda	Eocene	269.00	81.00
Pirkoh	Eocene	350.00	99.00
Sirki	Eocene	449.00	84.00
Habib Rahi	Eocene	533.00	143.00
Ghazij	Eocene	676.00	660.00
Sui Main Limestone	Eocene	1336.00	109.00
Ranikot	Paleocene	1445.00	363.00
Parh Limestone	Late Cretaceous/Early Cretaceous	1808.00	8.00
Upper Goru	Late Cretaceous/Early Cretaceous	1816.00	340.00
Lower Goru	Early Cretaceous	2156.50	1175.00

2.6 Petroleum Prospect

A successful petroleum system involves three key processes: hydrocarbon creation, movement, and accumulation in an appropriate trap. These activities take place within a framework of key geological features, including source rock, reservoir rock, seal rock, and trap. For a petroleum system to be successful, all of its components must be present in the right spatial and temporal order. In this context, Pakistan's Lower Indus Basin is a well-established and highly prolific petroleum area, notably in terms of natural gas. The basin contains thick sedimentary successions that have experienced adequate burial and thermal maturation, allowing for efficient hydrocarbon generation.

The Sembar Formation serves as the primary source rock, consisting of organic-rich marine shales that can produce hydrocarbons under the right conditions. The produced hydrocarbons migrate into the Lower Goru Formation, which serves as the primary reservoir due to its sandstone units' high porosity and permeability. The Upper Goru shales that cover these reservoirs effectively seal them off, preventing hydrocarbons from escaping upward. Hydrocarbons are primarily trapped in anticlinal structures and fault-related traps, which are prevalent across the basin. The combination of four elements is source, reservoir, seal, and trap along with effective generation and migration processes, has resulted in multiple profitable gas fields, notably the Miano Field. As a result, the Lower Indus Basin is known as a gas-prone region with a well-developed and efficient petroleum system, making it one of the country's most important hydrocarbon-producing locations.

To summarize

- **Source: -** Sembar Formation
- **Reservoir:** - Lower Goru Formation
- **Seal:** - Upper Goru Formation
- **Structure:** - Horst and Graben

CHAPTER 3

SEISMIC DATA INTERPRETATION

3.1 Introduction

Seismic data interpretation is a critical stage in seismic data analysis. This technique entails identifying and interpreting numerous underlying geological structures, including faults, folds, and stratigraphic features. The interpretation workflow normally begins with horizon marking, then fault identification, and finally integration into a base map. The interpreter then selects an acceptable time for each horizon in the study area. Velocity analysis is then used to calculate vertical and horizontal velocities of the desired horizons using velocity data obtained during processing. The combination of time and velocity data enables the conversion of time observations into depth. Finally, contour maps of time, depth, and velocity are created to provide a more detailed picture of the subsurface.

The seismic method is one of the most essential techniques used in the oil and gas sector for subsurface research because it provides a comprehensive and thorough picture of underground geological conditions. Seismic interpretation is crucial for understanding subsurface geology, and each stage of the interpretation process is geared to accomplish this goal. These processes are critical for geophysicists to identify and develop hydrocarbon opportunities.

Seismic interpretation is critical in hydrocarbon exploration, development, and production, although it is not the only factor involved. It is usually used with other relevant data to create a dependable structural and stratigraphic picture of the subsurface. This comprehensive method guarantees that interpretations adhere to recognized geological and geophysical concepts. As a result, reliable seismic interpretation is critical for effectively identifying and utilizing hydrocarbon resources (Herron, 2011).

3.2 Objectives

i. The primary goal is to interpret seismic data to identify subsurface geological features. This entails thoroughly analyzing seismic reflections to locate and map significant features like as faults, folds, and stratigraphic variations. This interpretation provides a clear grasp of the research area's subsurface geometry, which aids in the development of a dependable structural framework for the region.

ii. The second goal is to identify leads and opportunities for hydrocarbon accumulation.This is accomplished by creating and evaluating depth contour maps, which are supplemented by time contour maps from the Lower Goru, Sui Main Limestone, and Ranikot. The combination of these maps aids in understanding the underlying structural configuration and detecting probable trapping zones, reservoir units, and locations conducive to hydrocarbon accumulation.

3.3 Types of Seismic interpretation

Seismic stratigraphy, often known as stratigraphic interpretation, and structural interpretation are the two primary forms of seismic interpretation. Structural interpretation includes the identification and annotation of fault planes and horizons. Because the reflector is easily visible and because reflectors designate both sequence boundaries and the boundary with the reservoir, the interpreter follows the horizon over the reflector. The interpreter must then take note of faults, which are fractures or breaks in the subsurface rock that show movement. Knowing the vertical displacement is essential to prevent misinterpretation since one reflector occasionally continues over into another reflector above or below it, creating confusion (Bakker, 2002).

Based on the characteristics of the seismic data, stratigraphic interpretation entails observing and recording the stratigraphic changes as well as the location of these changes. These alterations can happen laterally and gradually. For instance, as one moves away from the source, a sandstone may gradually turn into a shale. Other alterations along the rock formation's bedding may also take place. Reflectivity and the wave trace vary as a result of these modifications (Sheriff, 2012).

3.4 Methodology

Kingdom Software was used for all of the procedures listed here. In order to create the base map, the workflow started with the loading of SEG-Y seismic data and navigation files. The control line portion was then identified and marked after well data were input. Then, to make well-to-seismic correlation easier, a synthetic seismogram was created. After that, fault and horizon picking were used for seismic interpretation. The Lower Goru Formation, Sui Main Limestone, Ranikot Formation, and Upper Goru Formation horizons were then shown on time and depth contour maps.

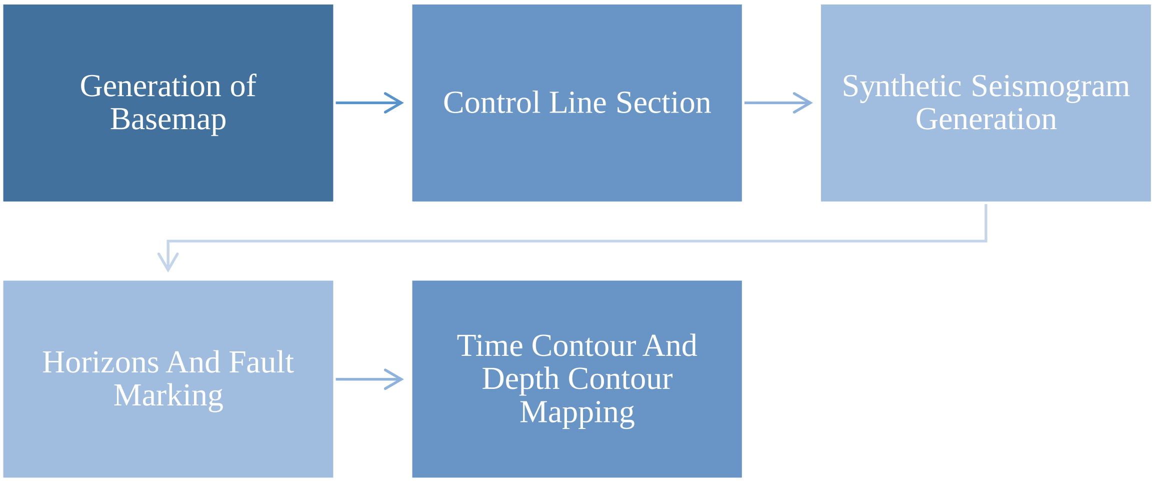

Figure 3.1 shows the entire seismic interpretation process, from basemap creation to time/depth contour map creation.

3.5 Generation of Base Map

After entering navigation files from the data originally accquired by OMV and later edited and converted by LMKR and adding SEG-Y files, the basemap was created using Kingdom software 2017. It displayed one strike line with a North South trend and four dip lines with an East West trend. Later, wells Miano 02 and 03 were added using information found in the well top data. A scale of 1: 349658 was used to depict the basemap.

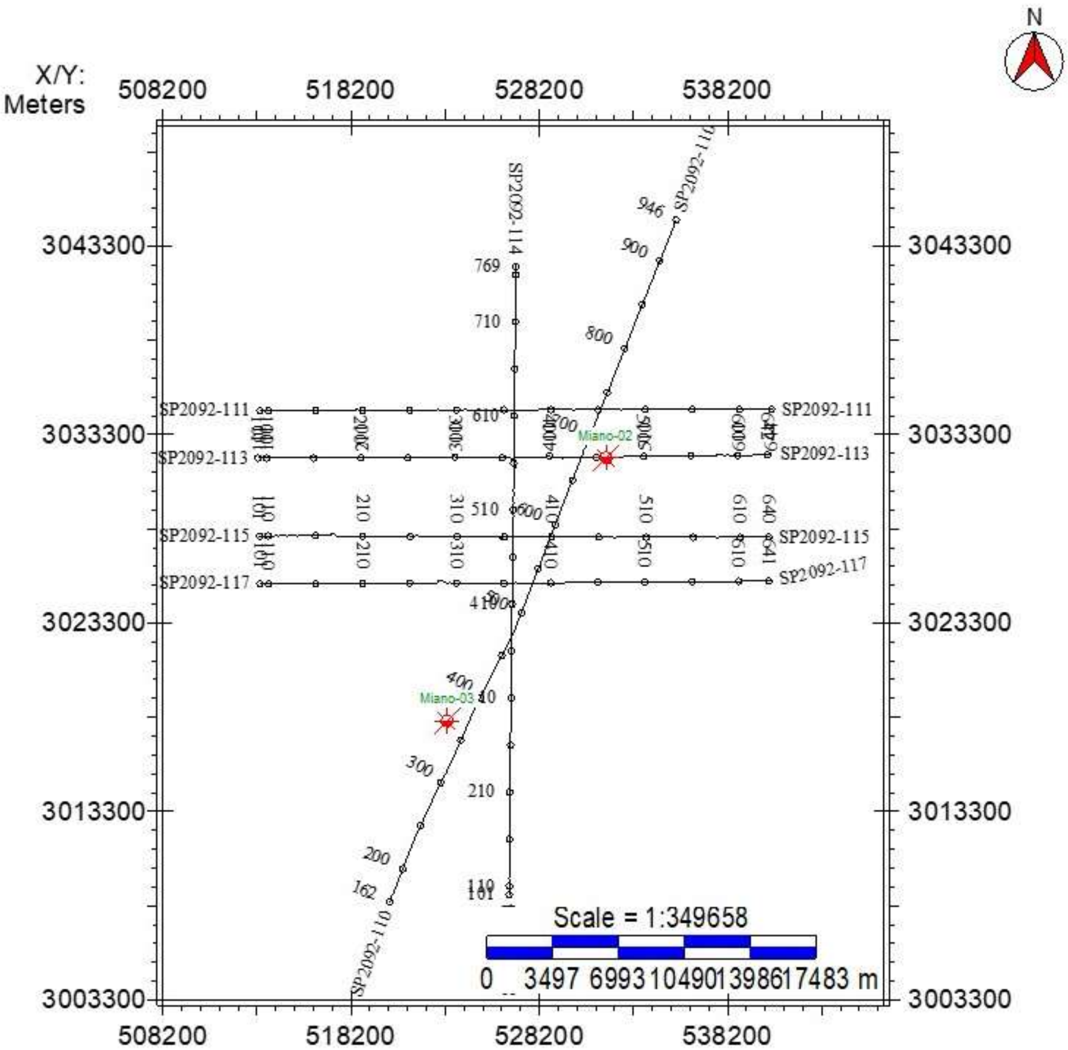

Figure 3.2 The generated base map of Miano area with lines at shot point interval of 1470 and wells displayed using Kingdom 2017 software. Scale of 1:1349658

3.6 Selection of Control line

Seismic line SP2092-114 was chosen as the control line for the seismic interpretation workflow since the Miano 02 well is situated on it at shot point 470.0. Because it is directly linked to well data via the synthetic seismogram, a control line is regarded as the reference seismic section and is the most dependable line for quality control and horizon calibration.

Faults and structural discontinuities were found along this line, and important seismic horizons were selected and connected with formation tops determined by the well tie. Since line SP2092-114 is the reference line, any inconsistencies, misties, or interpretation mistakes found in seismic picking or correlation on this line were initially fixed to guarantee consistency before extending interpretation to other lines in the survey.

Additionally, line SP2092-114 crosses the regional structural dip direction because it is an West-East orientated dip line. It is therefore especially useful for recognizing stratigraphic variations, fault geometry, and horizon continuity across the subsurface since it gives a clear picture of vertical structural variation. This dip-line control guarantees that the interpreted horizons are geologically consistent throughout the seismic volume and greatly increases the dependability of structural interpretation.

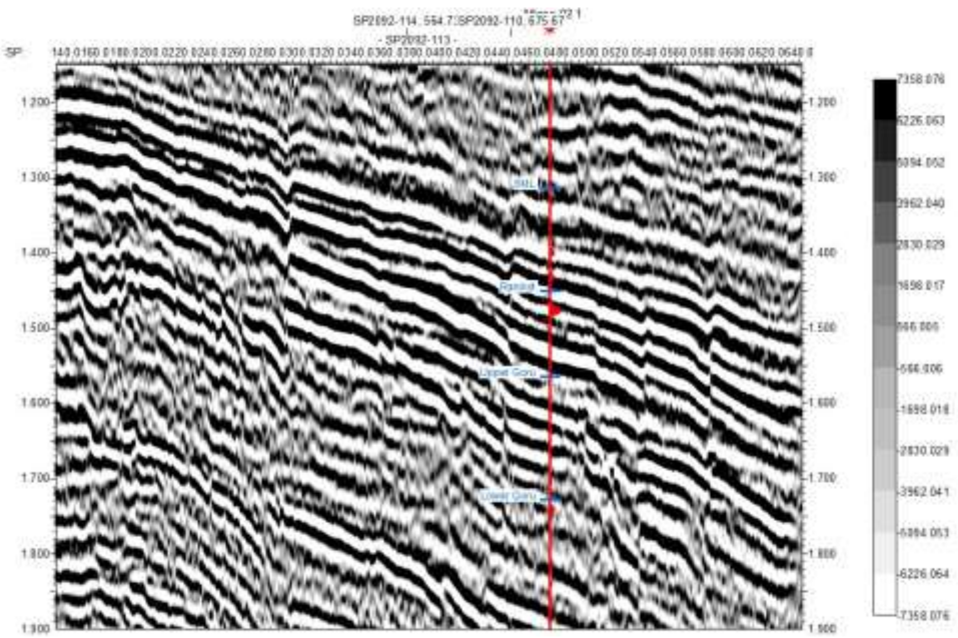

Figure 3.3 SP2092-114 Is the control line

3.7 Generation of a synthetic seismogram

Since it creates a trustworthy correlation between well data and seismic reflections, the creation of a synthetic seismogram is an essential step in seismic interpretation. The interpreter can precisely locate formation tops on seismic sections and ascertain the corresponding travel periods and depths thanks to this well-to-seismic linkage. The synthetic seismogram is an essential technique for improving horizon identification and lowering interpretation uncertainty by combining geological and geophysical data.

Using Kingdom 2017 software, artificial seismograms for the Miano 02 and 03 wells were created for this investigation. Using check-shot and velocity data from the well data, a time-depth relationship was first generated. To guarantee data quality, sonic and density logs were subsequently imported and conditioned. Bulk density measurements were taken from the density log, while compressional velocity values were obtained from the sonic log.

During the well-tying procedure, the gamma-ray log served as a reference for quality control and lithological correlation. The velocity and density measurements at each depth interval were then multiplied to determine the acoustic impedance. The acoustic impedance contrasts between neighboring layers were then used to calculate reflection coefficients, which produced a reflectivity series that represented variations in subsurface impedance. A representative seismic wavelet was taken from seismic traces near the wellbore in order to model the seismic response. The synthetic seismogram was created by convolving this extracted wavelet with the reflectivity series.

On seismic line SP2092-114, the synthetic seismogram for Miano 02 was produced at shot point 470. To determine important stratigraphic markers and create precise horizon ties, the generated synthetic trace was connected with the corresponding seismic section. The produced synthetic seismograms offered a trustworthy foundation for fault tracing, seismic horizon interpretation, and ensuing structural and stratigraphic investigation in the research region.

By guaranteeing that geological formation tops were accurately identified and connected across the seismic dataset, the successful well-to-seismic connection derived from these synthetic seismograms greatly increased the confidence of seismic interpretation. The mapping of significant reservoir and regional stratigraphic horizons, such as the Lower Goru, Upper Goru, Sui Main Limestone, and Ranikot formations, was made possible by this.

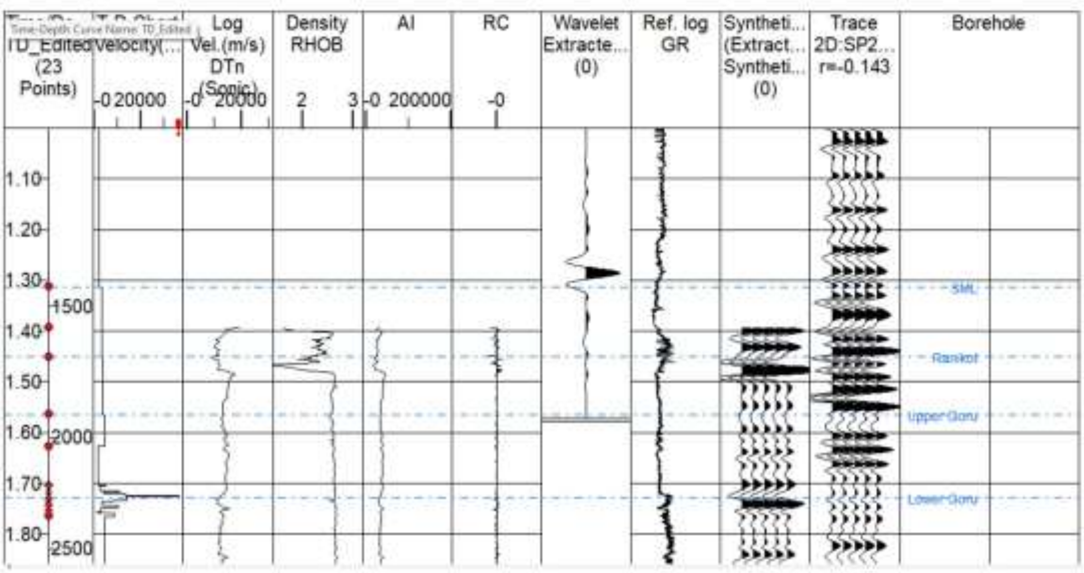

Figure 3.4 Synthetic seismogram of Minao 02 generated using kingdom software. The time of formations Ranikot, Sui Main limestone, Upper Goru and Lower Goru respectively is displayed in dotted blue

3.8 Interpretation of Seismic Lines

The selection and correlation of seismic horizons and faults constituted the subsequent phase of the interpretation procedure. In order to ensure precise matching between well tops and seismic reflectors, the control line was first loaded and important horizons corresponding to the Lower Goru Formation, Ranikot Formation, Upper Goru Formation and Sui Main Limestone were interpreted using the synthetic seismogram tie.

The interpretation was expanded to nearby and connected seismic lines after the horizons were determined on the control line. In order to preserve structural continuity between various sections, arbitrary lines were digitized throughout the 2D seismic survey grid. Horizon picks were transmitted from the control line to the nearby lines throughout this procedure, guaranteeing reflector identification uniformity throughout the dataset.

A manual bulk shift was used to correctly align the horizons when there was a discrepancy in the two-way transit time between intersecting seismic sections. This modification aided in clearing up errors and preserving a uniform seismic framework throughout the survey region. A more dependable and geologically consistent interpretation model was produced as a result of this iterative procedure, which also improved fault geometries and horizon continuity.

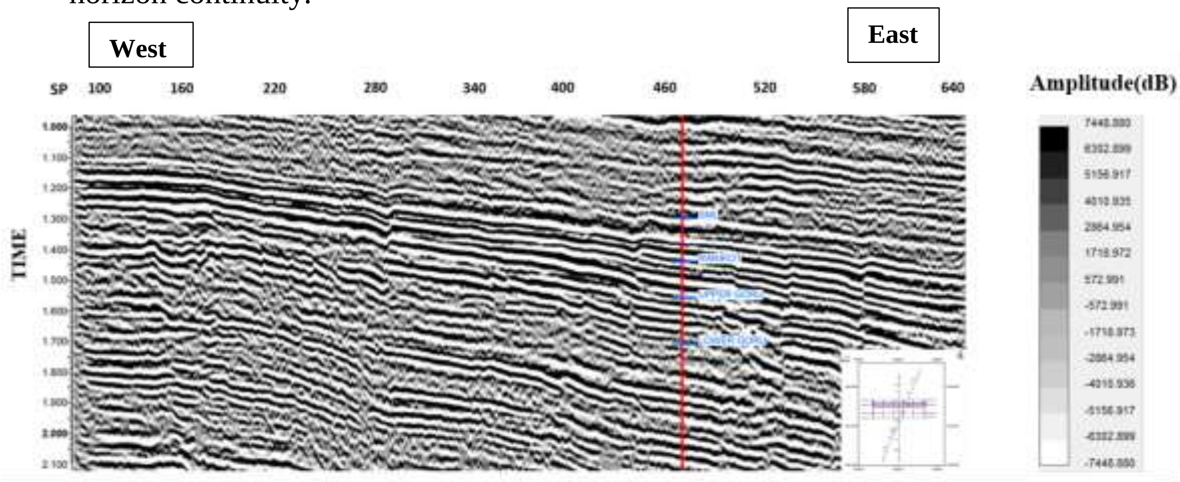

Figure 3.5 Uninterpreted Seismic control line SP-2092-113. The color bar is of amplitude with the white part having negative decibel values and the black part having positive decibel values

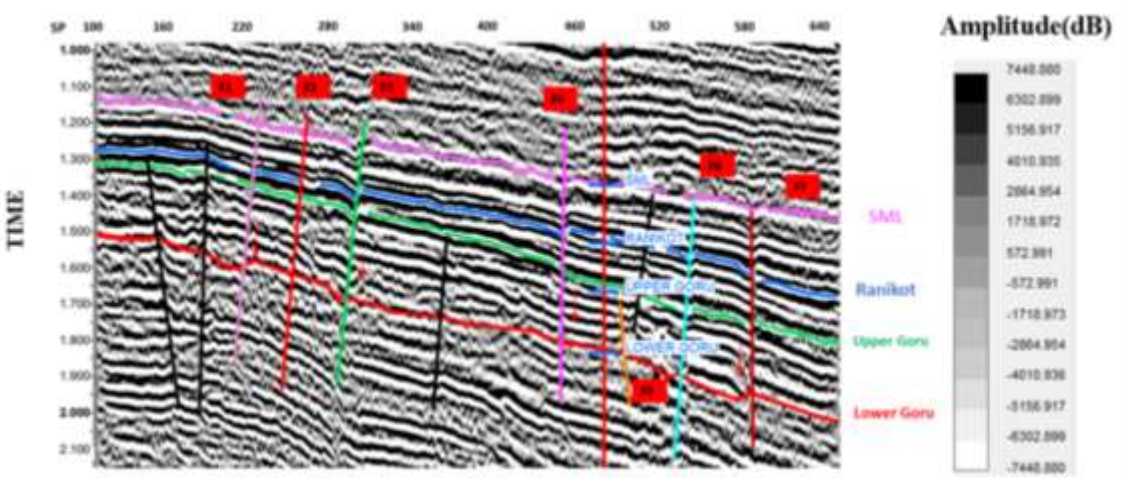

Figure 3 6 Interpreted Seismic control line SP-2092-113, a dip line with West to East trend with horizons Lower Goru(LG),Upper Goru, Sui Main Limestone(SML) and Ranikot.

SP-2092-113 is the control line dip line with West-East trend with the well Miano-02 situated on line at shotpoints 470.0. The faults are marked on horizon Lower Goru. The well is situated on a horst with the surrounding blocks being graben due to the downward movement of hanging wall. The trend is almost the same with most faults from Lower Goru reaching up to Sui Main. The color bar shows the amplitudes at each reflector with the black shade showing a higher amplitude and the red shade showing a lower amplitude, unit of amplitude is decibels (dB).

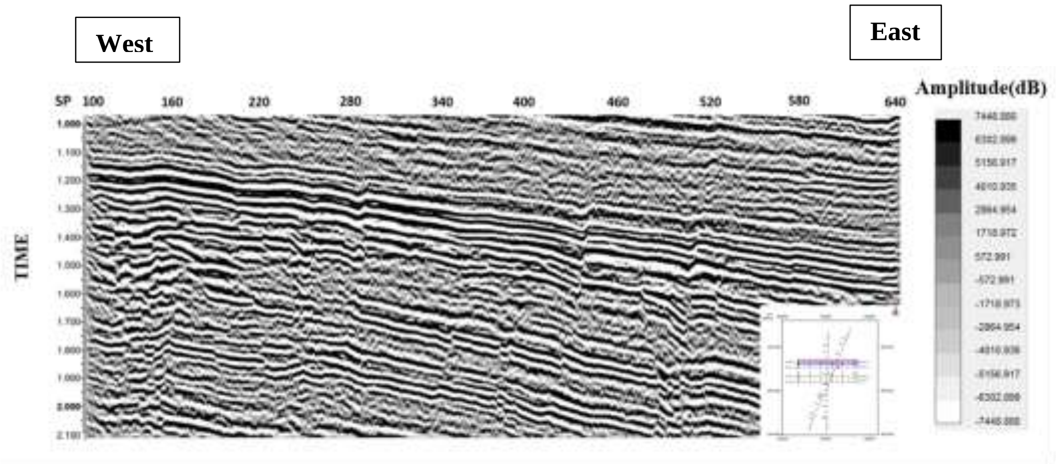

Figure 3.7 Uninterpreted Seismic line SP-2092-111, a dip line with West to East trend

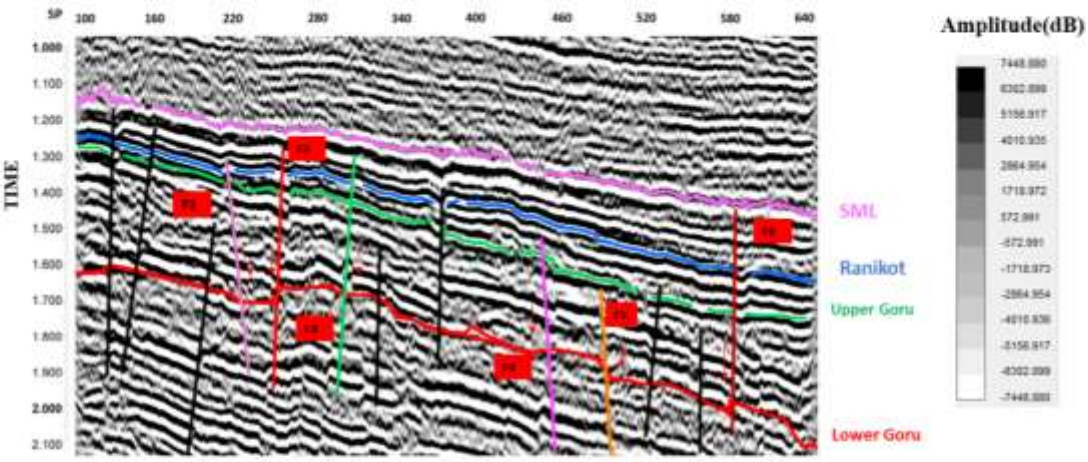

Figure 3.8 Interpreted seismic line SP-2092-111

The seismic line SP-2092-111 is the line parallel to control line SP-2092-113. It is also a dip line with West-East trend. As this line is parallel to the previous line it is showing almost the exact same trend of horst and graben and half graben with the correlated faults Sui Main Limestone formation, ranikot and upper goru formation with their respective horst and graben structure.

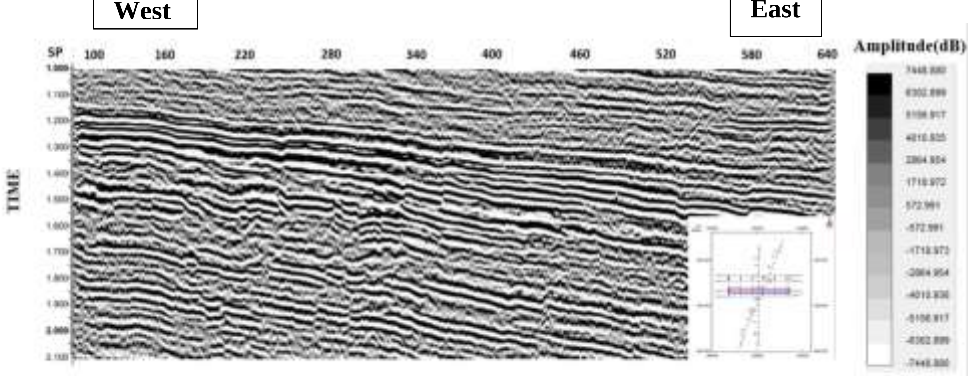

Figure 3.9 Uninterpreted Seismic line SP-2092-115, a dip line with West to East trend

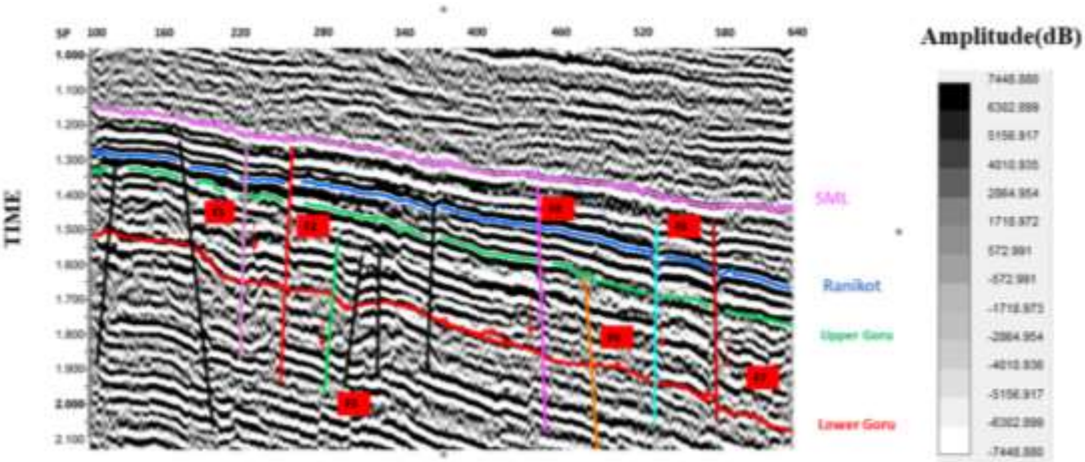

Figure 3.10 Interpreted seismic line SP-2092-115

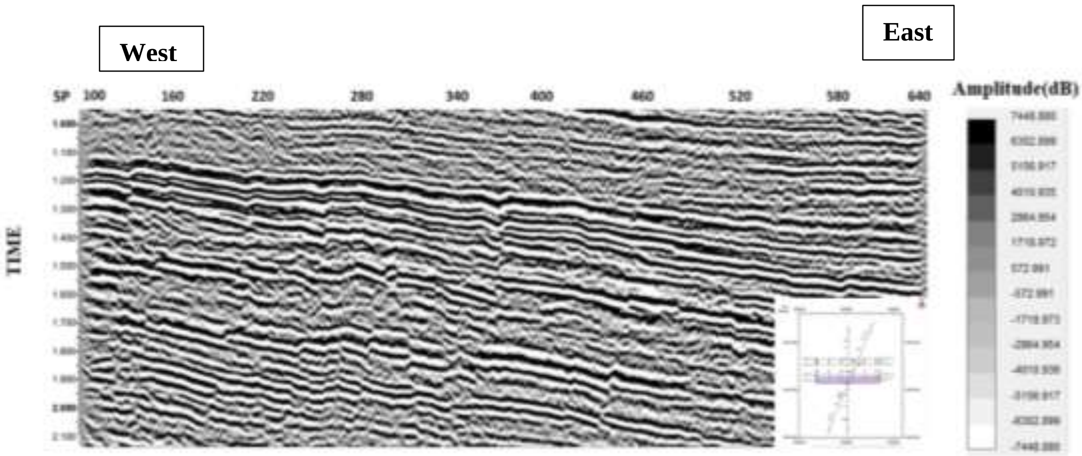

Figure 3.11 Uninterpreted Seismic line SP-2092-117, a dip line with West to East trend

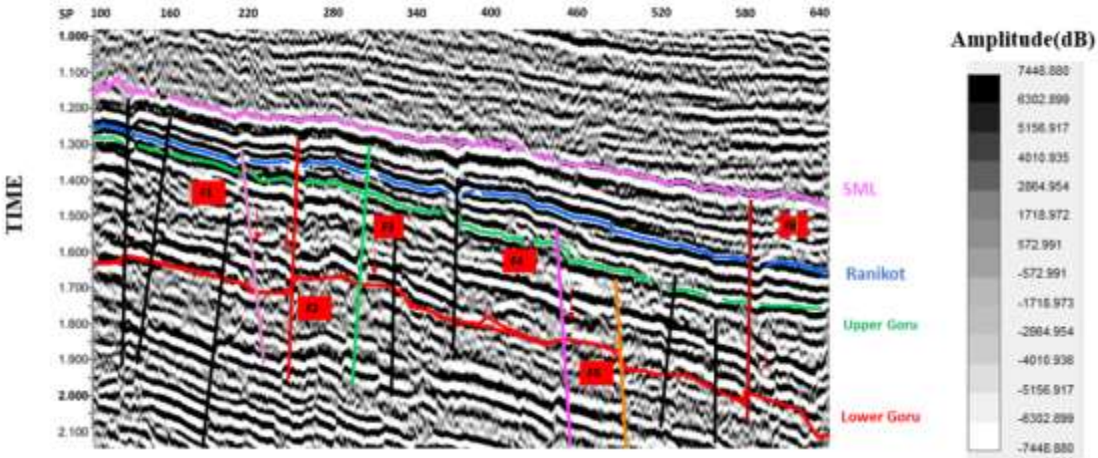

Figure 3.12 Interpreted seismic line SP-2092-117

All the seismic dip lines SP-2092-111, SP-2092-113, SP-2092-115 SP-2092-117 have more or less the same trend of correlated faults marked at

Lower Goru, Ranikot and Sui Main formation. The corelated faults were later used to create fault polygons.

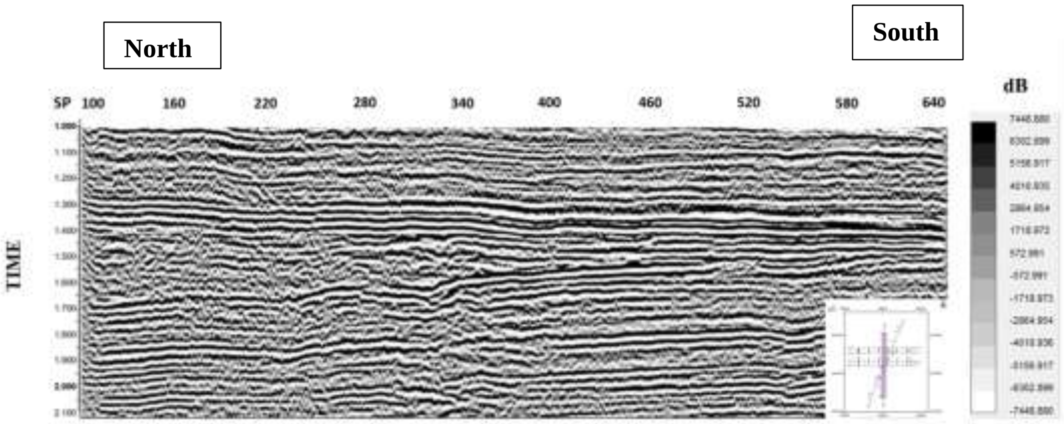

Figure 3.13 Uninterpreted Seismic line SP-2092-114, a strikeline with North-South trend

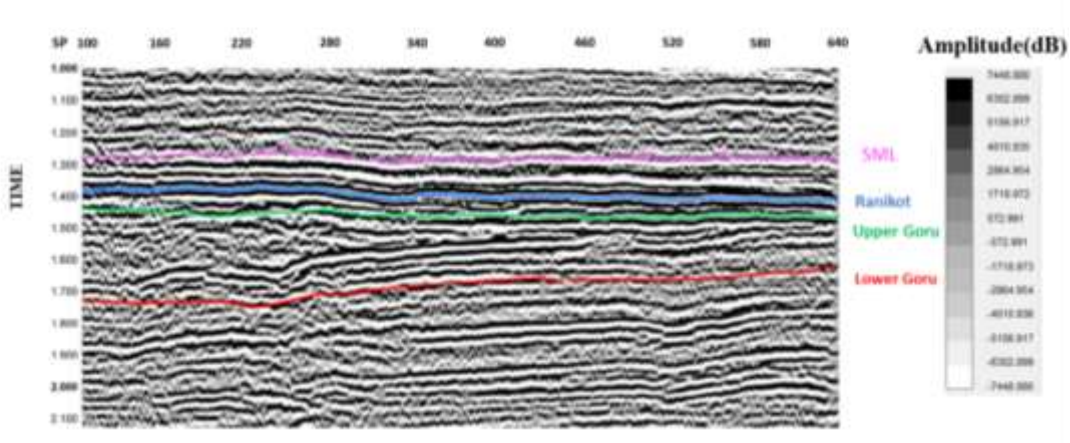

Figure 3.14 Interpreted seismic line SP-2092-114

The direction of the strike line is North-South and the structure is on a horst with the surrounding blocks being graben due to the downward movement of hanging wall. The trend is almost the same with most faults from Lower Goru reaching up to Sui Main and ranikot The color bar shows the amplitudes at each reflector with the black shade showing a higher amplitude and the red shade showing a lower amplitude, unit of amplitude is decibels (dB).

3.9 Seismic contouring

Seismic contouring is used to link the different features of seismic signals with the different structural forms of rock deformation. Using a computer to create maps in sets is easy (Tucker, 1988).

In geophysics and geological research, seismic countering is a special method. Over the years, geoscientists have extensively researched and acknowledged this method. This method involves mapping the underlying structures by examining the seismic waves that are reflected off various geological layers (Smith & Jones 2017).

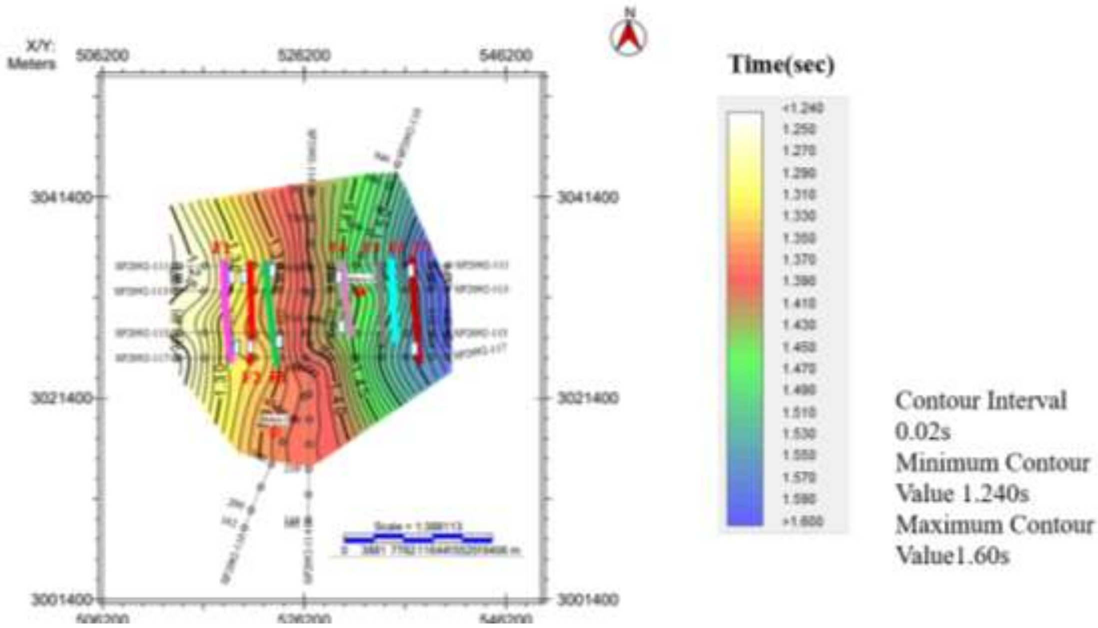

Figure 3.15 Time contour map of Ranikot Formation.

The colour bar represents the shallow level meaning it took less time to be reflected back. The time contour map for the Ranikot Formation was created by first generating the time grid for Ranikot horizon after the correlation of faults and the formation of fault polygons, then the contour was generated. The structure shown is horst and graben structure Ranikot time contour Map

Two-way travel time (TWT) map was generated to represent the time of Ranikot Formation for representation of relief features and faults. The higher values of the time represent the deeper level meaning it took more time for the seismic wave to be reflected back while the lower value of time through the fault polygons. The contour interval is kept at 0.02s and minimum contour value is 1.240s and maximum contour value is 1.60s.

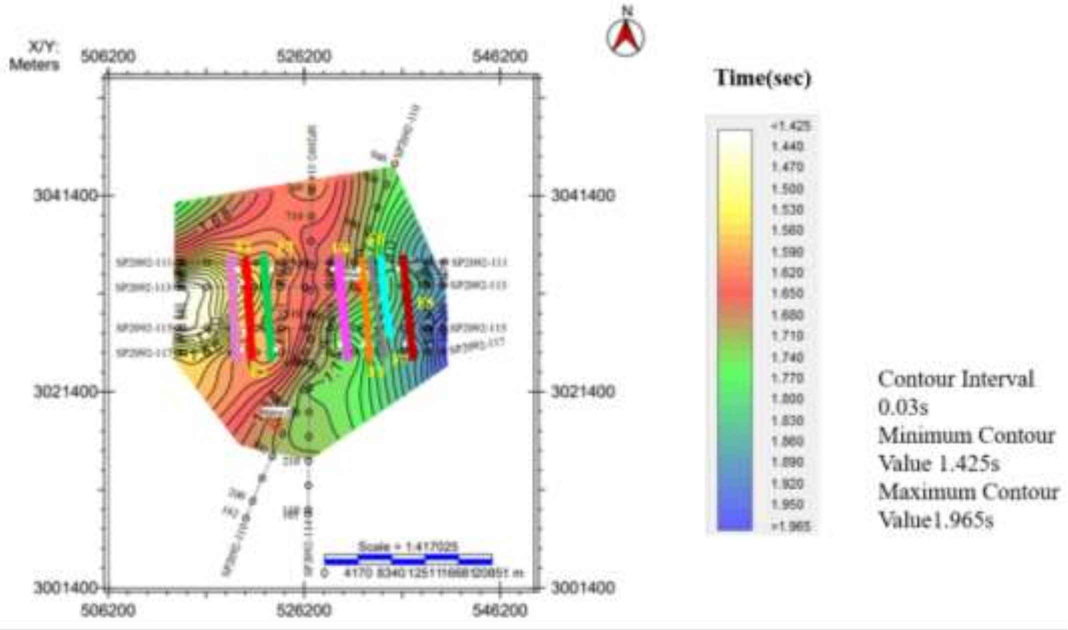

Figure 3.16 Time contour map of Lower Goru Formation.

The process of generating the time contour map of Lower Goru Formation was exactly the same as it was for Ranikot Formation. The contour interval was kept at 0.03s, the minimum contour value was 1.425 s and the maximum contour value was 1.965s

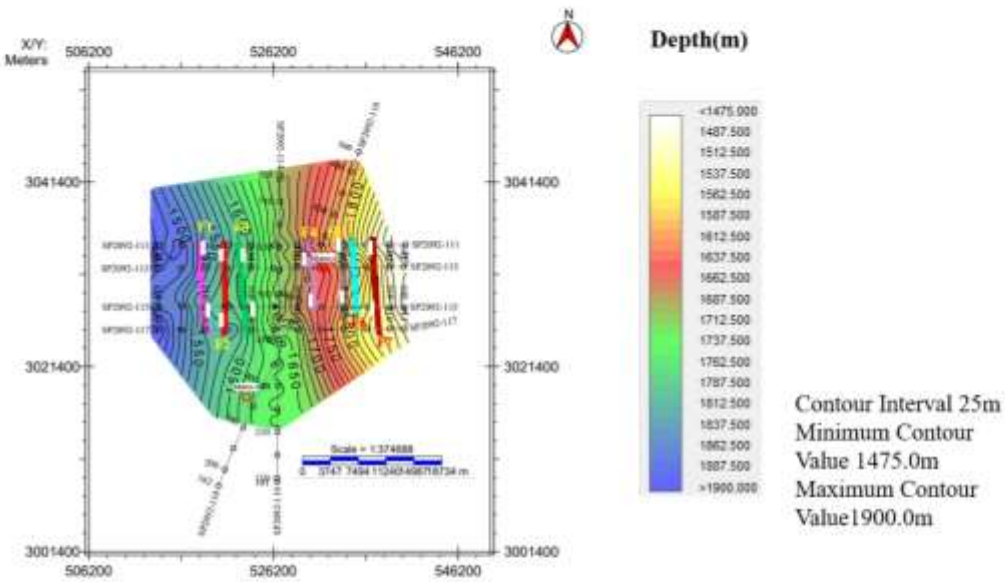

Figure 3.17 Depth contour map of Ranikot Formation.

The time map was converted into a depth map using the formula

$$S = \frac{V * T}{2}$$

The depth contour value of the well matches with the value of synthetic seismogram after that justifies the structural interpretation. The contour interval of Lower Goru depth is 25m, the minimum contour value is 1475m and maximum contour value is 1900m. The faults show horst and graben and half graben structure just like in the time contour map.

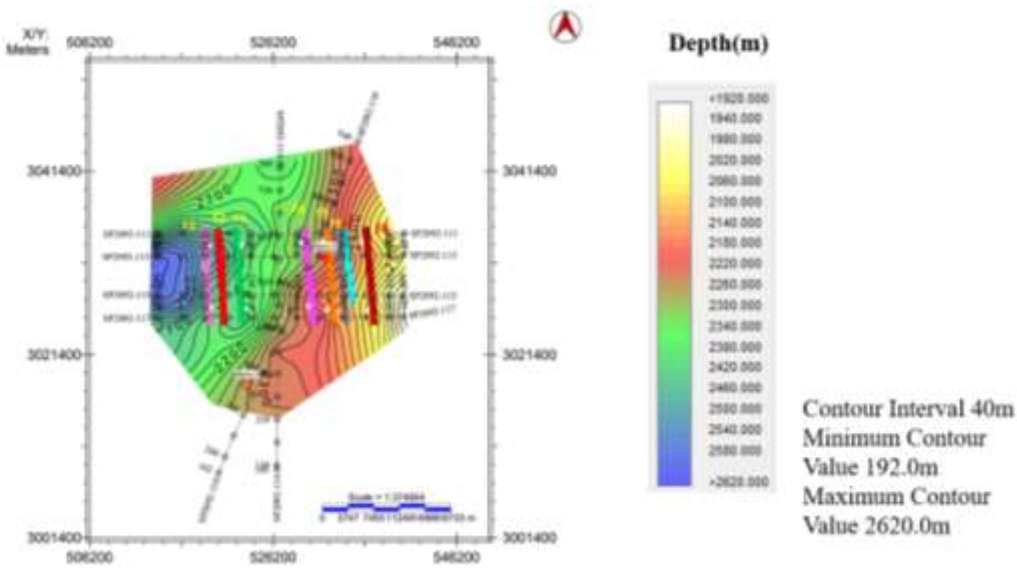

Figure 3.18 Depth contour map of Lower Goru Formation.

The contour value on the well matches with the value of synthetic seismogram that justifies the structural interpretation. The contour interval of Lower Goru Formation is 40m, the minimum color value of contour is 1920m and maximum is 2620m.

CHAPTER 4

PETROPHYSICAL ANALYSIS

4.1 Introduction

According to Islam et al. (2017), the petrophysical analysis focuses on the physicochemical characteristics of rocks and how they interact with fluids. Petrophysics is the study of physical properties of rocks using various petrophysical methods such as electric, nuclear, and acoustic sources, which are carried out using wireline logs to obtain well properties. Because reservoir rocks must have porosity and permeability, we are primarily interested in researching them to identify hydrocarbon-yielding zones. Several logging equipment are dropped into the borehole, providing information about the surrounding formations. Based on this information, reservoirs are examined to determine whether they are suitable for production, as well as testing and completion of a well.

Well logs offer real-time measures of porosity, lithology, and the existence of fluid in a formation. The information establishes the presence of hydrocarbons and other fluids, if any, as well as whether a rock is suited for containing such fluids. It also provides information on the borehole environment.

4.2 Log utilized for well interpretation

This is the initial step of petrophysical analysis, in which prospective reservoir zones are discovered using various well logs. Several key aspects must be considered for zone marking.

First, all logs are carefully examined, and formation tops are noted at the appropriate depths. Borehole size varies, but frequently increases in zones with loose shales or poorly compacted strata. A stable zone should have a consistent (in-gauge) caliper log, suggesting good drilling conditions.

Following that, the gamma ray log is evaluated to determine the shale content. Because reservoir rocks should have a low shale volume, zones with low gamma ray readings are regarded possible reservoirs, whereas high values suggest shale-rich areas.

Next, resistivity and porosity logs are evaluated together. Common resistivity logs include LLD (deep), LLS (shallow), and MSFL (micro), each with a distinct level of inquiry and scale. High resistivity levels typically indicate the presence of hydrocarbons, whereas low resistivity denotes water-bearing formations (particularly saline water).

When a prospective hydrocarbon zone is found using resistivity logs, porosity data (such as neutron and density logs) are also considered. In clear formations, the neutron and density curves intersect, indicating water-filled zones. However, in gas-bearing zones, a crossover effect (separation of curves) is seen, which is a useful hydrocarbon indicator.

4.2.1 Porosity Log

A porosity log is a type of well log used to determine the porosity of subterranean rock formations, or the percentage of the rock's volume made up of pore spaces that may hold fluids such as water, oil, or gas.

4.2.1.1 Density porosity

Density porosity is deemed reliable only when drilling conditions are typical and there is no caving or washout. Without such optimal conditions, density porosity cannot be used effectively since the data may be inaccurate or unreliable for interpretation. To overcome this limitation, sonic porosity is used, and an average porosity is determined from sonic measurements. The procedure for estimating density porosity is commonly used when the borehole environment is steady and devoid of problems like caving or washout (Ellis & Singer, 2007).

The following formula is used to calculate density porosity:

$$\varphi D = \frac{\rho ma - \rho b}{\rho m - \rho f} \qquad \textbf{4.1}$$

φD = Density porosity of the rock.

ρma = Density of the rock matrix (2.65 g/cm3).

ρb = Bulk density of the formation (log response in the one of interest).

ρf = Density of the fluid occupying the pores (1.1 g/cm3).

4.2.1.2 Neutron porosity

The neutron log data from the depth of interest can be utilized to calculate neutron porosity. The neutron log provides an accurate representation of porosity.

4.2.1.3 Sonic porosity

Sonic porosity is another way to measure the porosity of a rock formation in petrophysics. It is based on the measurement of acoustic wave travel time through rock (Serra, 1984).

$$\varphi s = \frac{\Delta t log - \Delta t ma}{\Delta t f - \Delta t ma} \qquad \textbf{4.2}$$

φs = Sonic porosity

$\Delta t log$ = Transit time in the formation of interest.

$\Delta t ma$ = Transit time through 100% of the rock matrix.

$\Delta t f$ = Transit time through 100% of the pore fluid.

4.2.1.4 Average porosity

Average porosity is the average of density and neutron porosity and the formula used is written below:

$$\Phi T = \frac{\Phi D + \Phi N}{2} \qquad \textbf{4.3}$$

φ_A= Average Porosity.

φ_D= Density Porosity.

φ_N= Neutron Porosity.

4.2.1.5 Effective porosity

The Sonic Porosity Log estimates effective porosity, which is the volume of linked pore spaces within the rock that allow fluid to flow.

4.2.2 Lithology Log

A lithology log, a type of well log, records the types of rocks (lithology) discovered in a borehole, which are often obtained via core samples, well cuttings, or data interpreted from other geophysical logs.

4.2.2.1 Gamma log

Identifies natural radiation to aid in distinguishing between shale (high radioactivity) and non-shale rocks (low radioactivity).

4.2.2.2 Spontaneous Potential

Identifies the intrinsic electrical potential changes between the wellbore and the formation. It is subject to lithological and permeability fluctuations..

4.2.2.3 Resistivity log

The formation's resistance to electrical current flow is determined by its lithology, porosity, and pore fluid resistivity.

4.2.2.4 Density

Determines the formation's bulk density, which reveals its porosity and rock matrix. It's very useful for identifying different lithologies.

4.2.2.5 Sonic log

Calculate the velocity of sound waves as they pass through the formation, taking into account lithology and porosity. They are used to determine porosity and discriminate between different rock types.

4.2.3 Fluid Log

A fluid log is a well log that helps identify and describe the types of fluids (such as oil, gas, or water) present in the pore spaces of a rock formation.

4.2.3.1 Resistivity log

The electrical resistivity of rocks and formations within a well can be measured using resistivity logging, also known as electrical well logging. This measurement helps to determine reservoir properties, locate hydrocarbon zones, and characterize the subsurface.

4.2.3.2 Spontaneous Potential (SP)

This log measures the inherent potential difference between the drilling fluid and the surrounding rock. Its primary use is to distinguish between different lithologies (such as sandstones and shales) and to identify permeable zones.

4.2.3.3 Sonic Log

This log indicates how long it takes for sound waves to travel through the rock. The elastic properties of the rock, which are influenced by lithology, porosity, and pore fluids, are directly linked to the transit time.

4.2.3.4 Resistivity of water (Rw)

To determine fluid saturation, you must first know the resistivity of the water. Water resistivity can be determined using the picket plot approach, the SP method, or direct computation using the equation.

4.2.3.5 Picket plot creation

The Pickett plot below is created with porosity and resistivity values acquired from well log data. Porosity is represented on the x-axis, while resistivity is plotted on the y-axis using a logarithmic scale. The plot is used to examine reservoir characteristics and calculate water saturation. A water line (Sw = 100%) is used to distinguish between water- and hydrocarbon-bearing zones. Data points that deviate from the water line may indicate the presence of hydrocarbons, whereas points near to the line show water-saturated zones. This graphic aids in determining reservoir quality and locating productive intervals within the formation.

4.2.5 Saturation Of Water (Sw)

It calculates the quantity of wet zone in the given area of interest. It can be calculated with the following formula:

$$Sw = \sqrt{Rw/\,Rt \times 1/\,\phi e\,2} \qquad 4.4$$

Where;

Rw = Resistivity of water

Rt = True resistivity

Øe = Effective porosity

4.2.6 Saturation Of Hydrocarbon

The following formula is used to compute hydrocarbon saturation based on water saturation in the zone of interest:

$$Sh = 1 - Sw \qquad 4.5$$

Where;

Sh = Hydrocarbon saturation

Sw = Water saturation

4.3 Methodology for performing interpretation

The following methodology is used in the research area to emphasize the relevant information and parameters necessary for conducting this petrophysical analysis. The methodology employed in the research domain emphasizes the key information and parameters required for conducting this petrophysical investigation.

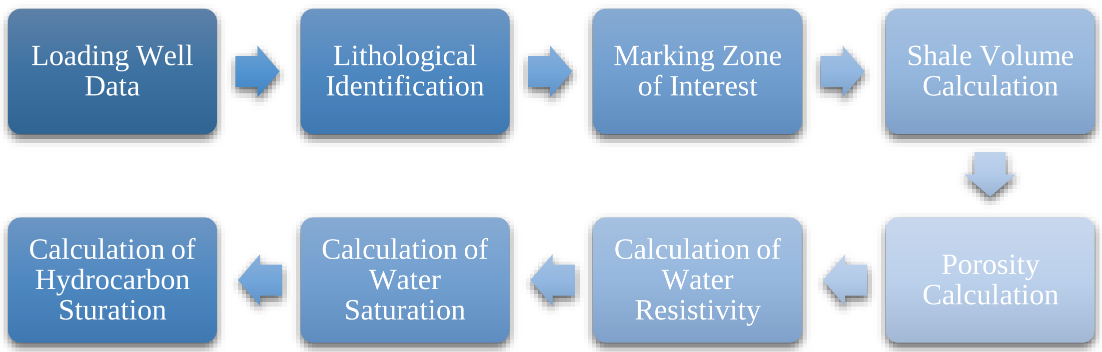

Figure 4.1 Complete Workflow of Petrophysical Analysis

The methodology employed in the research domain emphasizes the key information and parameters required for conducting this petrophysical investigation.

Petrophysical analysis is used in the oil and gas industry to discover possible oil or gas reserves and better understand subsurface rock formations. There are certain protocols to follow when performing petrophysical analysis. First, load the log data that we need to collect and organize from well logs. These logs record the geological formations discovered during well drilling. Using the log data, you may now identify several types of subsurface rocks, such as shale or sandstone.

Now that we've discovered the types of rocks, we can figure out certain properties like shale volume, porosity, water resistivity, water saturation, and hydrocarbon saturation. Before moving on to the next phase, ensure that the data is accurate and converted to normal scale units. Conduct a Formation assessment, which entails finding the most likely rock strata that may hold oil or gas. This is accomplished by looking for clues in the log data, such as a low gamma-ray log response (which could indicate less shale), variations in resistivity values, and other significant markers.

All of these approaches can be used to assess the potential for oil or gas production in specific geological layers, such as the Lower Goru Interval in the research region (Ellis and Singer, 2007).

4.4 Well interpretation of Miano-02 & 03

The Lower Goru Formation is drilled for petrophysical investigation using the Miano-02 & 03 well, which is situated in the Middle Indus Basin. Determining the two volumes—the shale volume and the clean volume is the first stage in the procedure. Neutron porosity, density porosity, average porosity, and effective porosity are among the porosity metrics that come next. Finally, fluid saturation is completed. Each of these characteristics is calculated using different well log curves employed in this investigation. I selected the Cretaceous-aged Lower Goru to evaluate its hydrocarbon potential for the petrophysical examination in our study.

4.4.1 Zone of interest & criteria

The interval chosen for hydrocarbon evaluation is known as the Zone of Interest (ZOI). Within this timeframe, well logs are analyzed to identify possible hydrocarbon-bearing reservoir zones and assess reservoir quality. The identification of productive reservoirs is based on a comprehensive review of multiple petrophysical logs. The primary criteria for reservoir identification are listed below.

4.4.1.1 Stable Caliper Log

A stable caliper log is required for accurate hydrocarbon evaluation because it indicates suitable drilling conditions and tool contact with the formation. Excessive borehole expansion or washout may affect the responses of density, neutron, and other formation-sensitive logs, leading to incorrect interpretations. Clean and competent deposits typically have steady caliper readings, whereas shale intervals frequently create washouts.

4.4.1.2 Clean Lithology with Low Gamma Ray Response

Reservoir zones are typically associated with clean sandstone or carbonate rocks with little shale content. The Gamma Ray (GR) log is used to distinguish between clean formations and shale intervals. Low GR values that shift toward the sand baseline suggest clean reservoir rock with increased porosity and permeability, whereas high GR values imply shale-rich, non-reservoir formations.

4.4.1.3 High Resistivity Response

Resistivity logs are important in hydrocarbon identification because hydrocarbons are more electrically resistant than saline formation water. Hydrocarbon-bearing zones typically have high deep resistivity values, which are often bigger than shallow resistivity readings due to mud filtrate invasion near the borehole. The separation of shallow and deep resistivity curves is considered a strong indicator of hydrocarbon presence.

4.4.1.4 Neutron–Density Crossover

The neutron and density logs are read combined to determine the fluid type and reservoir porosity. In water-bearing strata, both curves often overlap, however in hydrocarbon-bearing periods, particularly gas zones, the neutron and density curves cross over noticeably. This crossover phenomenon is regarded as a reliable measure of gas saturation within the reservoir.

4.4.1.5 Sonic Log and Interval Transit Time (DT)

The sonic log records the interval transit time (DT) of acoustic waves across the formation. Higher DT values indicate lower acoustic velocity, which often corresponds to higher porosity formations. Hydrocarbon-bearing zones, particularly gas reservoirs, frequently have elevated DT values due to lower formation density and enhanced compressibility. When combined with other log answers, the sonic log helps to establish reservoir quality and hydrocarbon occurrence.

Table 4. 1 The potential zone, starting, ending depth of Miano-02 Well.

Zone Of Interest-02				
Potential Zone	Producing Zone	Depth Start(m)	Depth End(m)	Total Depth(m)
Zone 1	Lower Goru	3533	3560	27

Table 4. 2 The potential zone, starting, ending depth of Miano-03 Well.

Zone of Interest-03				
Potential Zone	Producing Zone	Depth Start(m)	Depth End(m)	Total depth(m)
Zone 1	Lower Goru	3242	3279	37
Zone 2	Lower Goru	3413	3430	17

4.5 Petrophysics of Miano-02 and Miano 03

Petrophysics was performed; zones of interest were marked, and then picket plots for Miano 02 were generated.

The depth interval of 3490 m to 3560 m was chosen for detailed and comprehensive examination of the Miano-2 well's petrophysics. Raw log curves in a 7-track well log display show the basic recorded responses from various logging equipment and are used to undertake detailed petrophysical investigations of reservoir formations.

Track 1 shows the logs for Gamma Ray (0-200 API) and Caliper (6-16 inches). The gamma ray log identifies lithology by detecting natural radioactivity; high levels indicate shale, whereas low levels indicate clean sandstone or carbonate formations. The caliper log measures borehole diameter and can indicate washouts or stable formation zones.

Track 2 uses resistivity logs (0.2-2000 ohm•m) to calculate fluid content. Low resistivity suggests water-bearing zones, but high resistivity indicates the presence of hydrocarbons. Comparing the curves can aid in determining invasion effects and reservoir borders.

Track 3 shows porosity logs, including neutron porosity (NPHI: -0.15 to 0.45) and density log (RHOB: 1.9–2.9 g/cc). These logs are used to evaluate porosity, and their crossing or separation clearly indicates gas zones.

Track 4 contains the sonic log (DT/DLT), which measures acoustic transit time (0-100 or 140-350, depending on the scale) and helps estimate porosity and spot changes in rock compaction and fracture.

Track 5 displays the volume of shale (Vsh), which ranges between 0 and 1, with low values suggesting clean reservoir rocks and high values indicating shale-rich non-reservoir zones.

Track 6 contains porosity values such as total porosity (PHIA: 0-0.3) and effective porosity (PHIE: 0-0.3 to 0), with the latter being more important because it shows connected pore spaces available for fluidflow.

Finally, Track 7 illustrates water saturation (Sw: 0-1), which denotes the proportion of pore space filled with water; low Sw values indicate hydrocarbon-bearing zones, whereas high values indicate water-bearing formations. These seven tracks work together to provide a thorough interpretation of lithology, porosity, fluid type, and reservoir quality, allowing for more reliable hydrocarbon assessment.

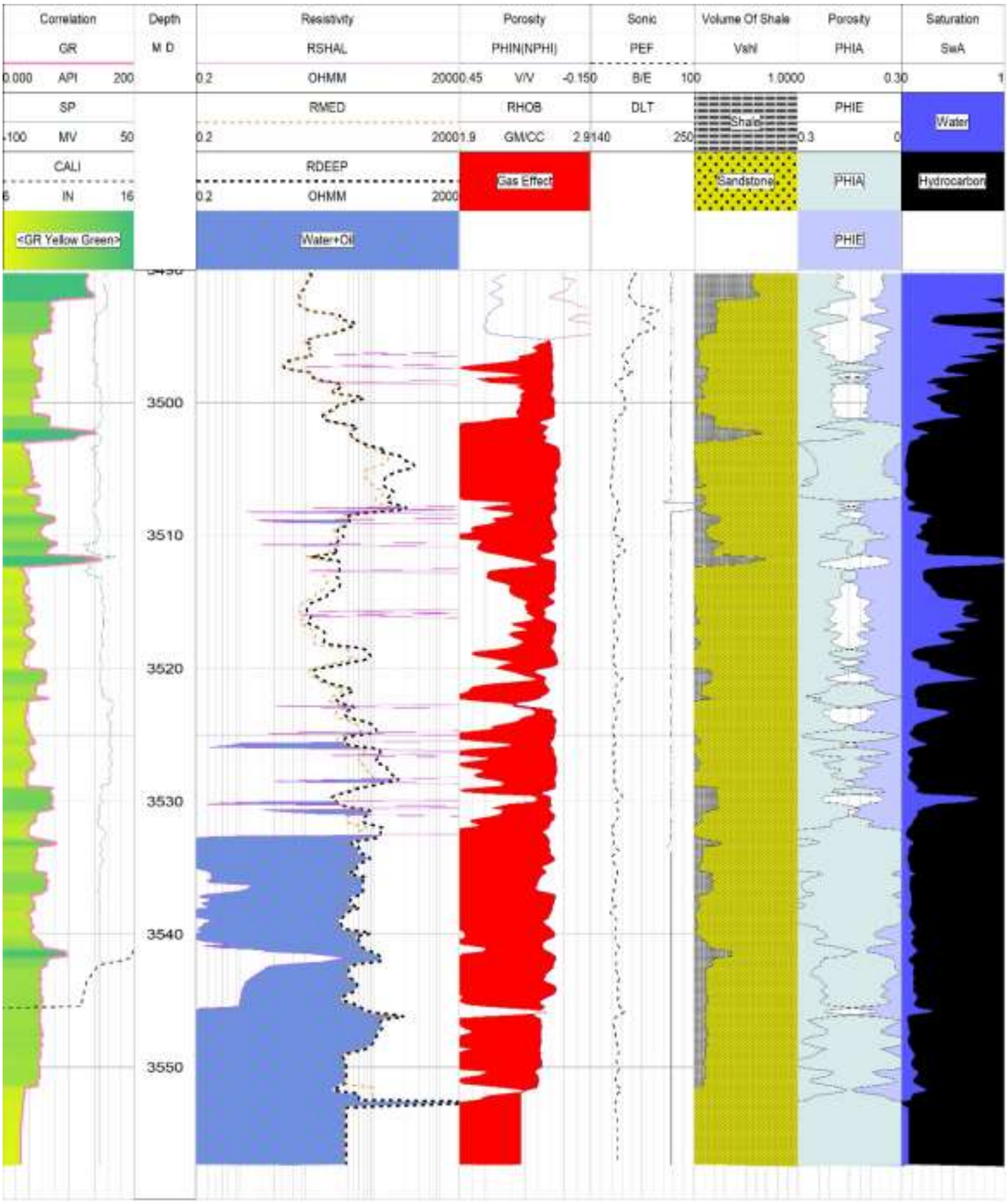

Figure 4.2 Uninterpreted, raw log curves of Miano Well -02

Petrophysics was performed; zones of interest were marked, and then picket plots for Miano 03 were generated. The depth interval of 3220 m to 3420 m was chosen for detailed and comprehensive examination of the Miano-3 well's petrophysics.

Different well log curves were organized into seven tracks to determine lithology, shale content, porosity, permeability indicators, and hydrocarbon saturation within the reservoir zone. Each track provides valuable subsurface information for reservoir characterization.

Track 1 includes the Gamma Ray (GR), Spontaneous Potential (SP), and Caliper (CALI) data. The Gamma Ray log was plotted on a scale of 0-200 API and is mostly used to discern between shale and clean sandstone deposits. High GR values imply shale-rich intervals, whereas low GR values indicate pure sandstone zones. The Spontaneous Potential log, which ranges from -100 to +50 mV, aids in finding permeable structures and their borders. The Caliper log, which measures borehole diameter on a scale of 6-16 inches, is used to detect borehole washouts or caving zones that could impair log quality.

Track 2 displays the resistivity logs, which include MSFL (Micro Spherically Focused Log), LLS (Laterolog Shallow), and LLD (Laterolog Deep), all shown on a logarithmic scale ranging from 0.2 to 2000 ohm-m. These logs are used to assess the fluid distribution inside the formation. The shallow resistivity logs look into the invaded zone near the borehole, whereas the deep resistivity log determines the true formation resistivity. The separation between shallow and deep resistivity curves frequently suggests the presence of hydrocarbons.

Track 3 contains the porosity logs, namely Neutron Porosity (NPHI/PHIN) and Bulk Density (RHOB).The Neutron Porosity log spans from 0.45 to -0.15 v/v, and the Density log from 1.9 to 2.9 g/cm^3. These logs are used combined to calculate formation porosity and determine lithology. In hydrocarbon-rich clean sandstone formations, a crossing of neutron and density curves may indicate gas-bearing zones.

Track 4 features the Sonic log (DTLB) with a range of 40-140 μs/ft. The sonic log monitors the time it takes for acoustic waves to move through the formation and can be used to determine compaction, lithology, and porosity. Higher transit time values typically suggest porous or less compact materials.

Track 5 plots the Volume of Shale (Vsh) from 0 to 1. This track is used to distinguish shale and sandstone intervals throughout the reservoir. Low Vsh levels imply cleaner sandstone formations, while high Vsh values denote shale-rich zones. The shale volume was mostly determined using the Gamma Ray log response.

Track 6 shows the porosity curves, which include Average Porosity (PHIA) and Effective Porosity (PHIE), both shown between 0 and 0.5. Average porosity is the formation's total porosity, whereas effective porosity is the number of linked pore spaces available for fluid movement after eliminating shale effects. These porosity records are useful for determining reservoir quality.

Track 7 displays the Water Saturation (Sw) plotted from 0 to 1, as well as hydrocarbon indicator curves. This track is used to determine the reservoir's fluid content. Low water saturation values reflect the existence of hydrocarbons, whereas high water saturation values indicate water-bearing formations. Hydrocarbon-bearing zones are found when water saturation drops dramatically within clean and porous sandstone intervals.

Overall, the integration of these seven log tracks yields a full picture of lithology, shale distribution, porosity, resistivity characteristics, and fluid saturation inside the Miano-3 well's selected interval. The combined interpretation aids in identifying prospective hydrocarbon-bearing reservoir zones and assessing reservoir characteristics.

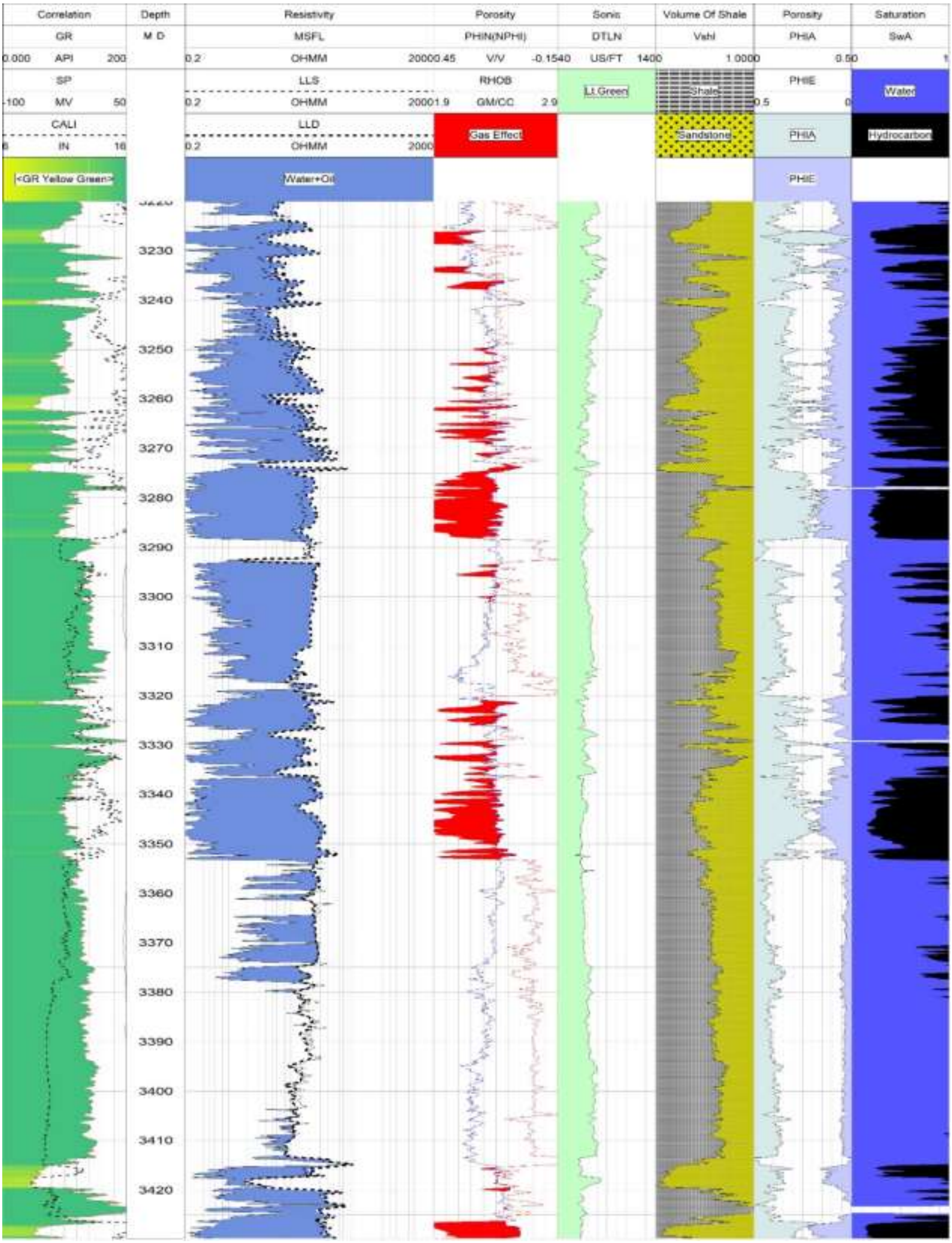

Figure 4.3 Uninterpreted, raw log curves of Miano Well -03

4.6 Marking Zone

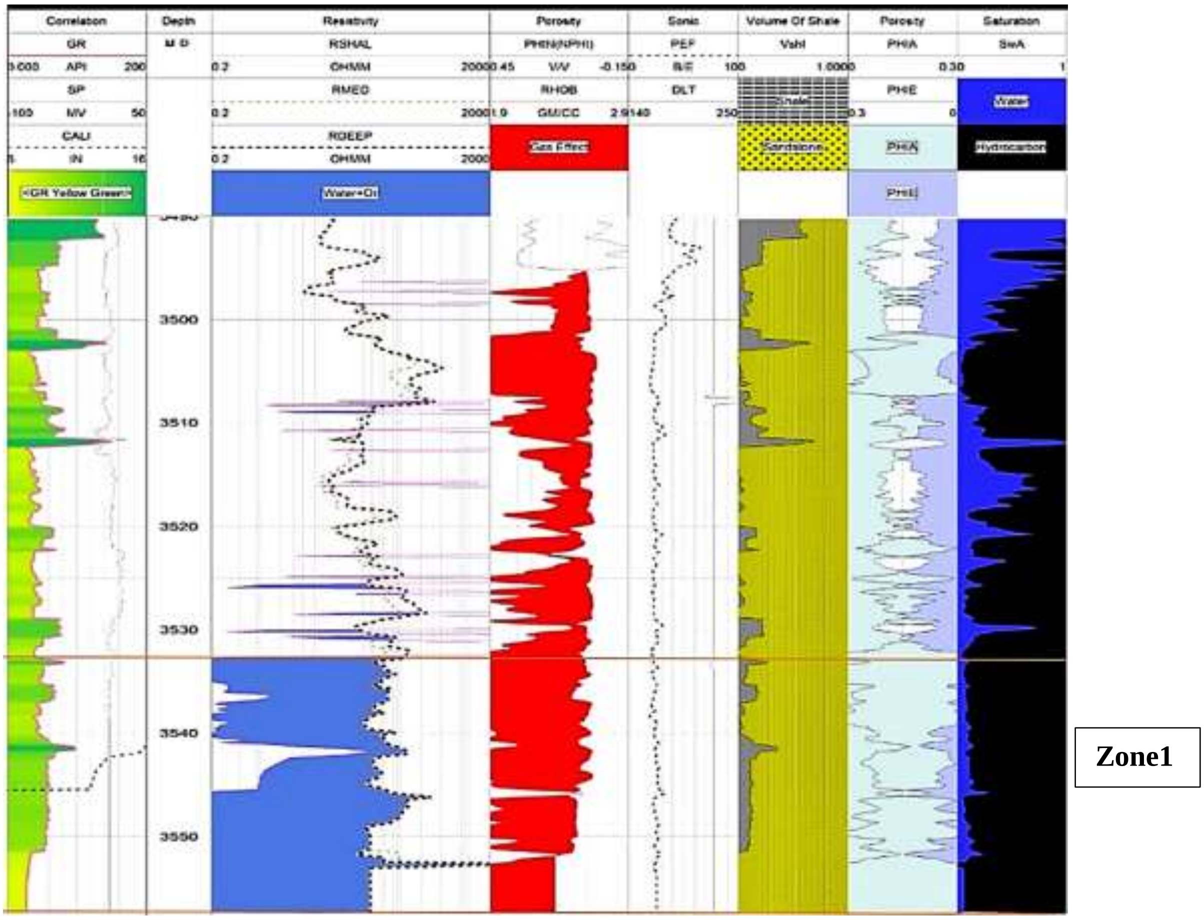

Figure 4. 4 Interpreted raw log curves of Miano 02 Well.

Table 4.3 Calculated parameters of Zone 1 (Miano 02 well)

Zone 1		
Depth	3495-3558	**Average (%)**
Vsh	0.12	12
PHIA	0.27	27
PHIE	0.24	24
Swa	0.92	92
Sw	0.8	8

Zone 1 is identified as a prospective hydrocarbon-bearing reservoir based on the combined response of many well logs. The caliper log remains stable, suggesting proper borehole conditions and consistent log readings. The gamma ray log has low values and shifts toward the sand baseline, indicating a clean sandstone formation with low shale concentration. The resistivity logs show significant deep resistivity values and a clear distinction between shallow and deep resistivity curves, indicating hydrocarbon saturation inside the uninvaded zone.

Furthermore, the neutron and density logs indicate a distinct crossover effect, indicating the likely presence of gas hydrocarbons. The sonic log also shows comparatively high DT values, indicating better porosity and lower acoustic velocity, both of which are desirable reservoir features. Zone 1 is considered as a good-quality hydrocarbon-bearing reservoir interval based on the combination of steady caliper conditions, low gamma ray response, high resistivity, neutron-density crossover, and increased DT values.

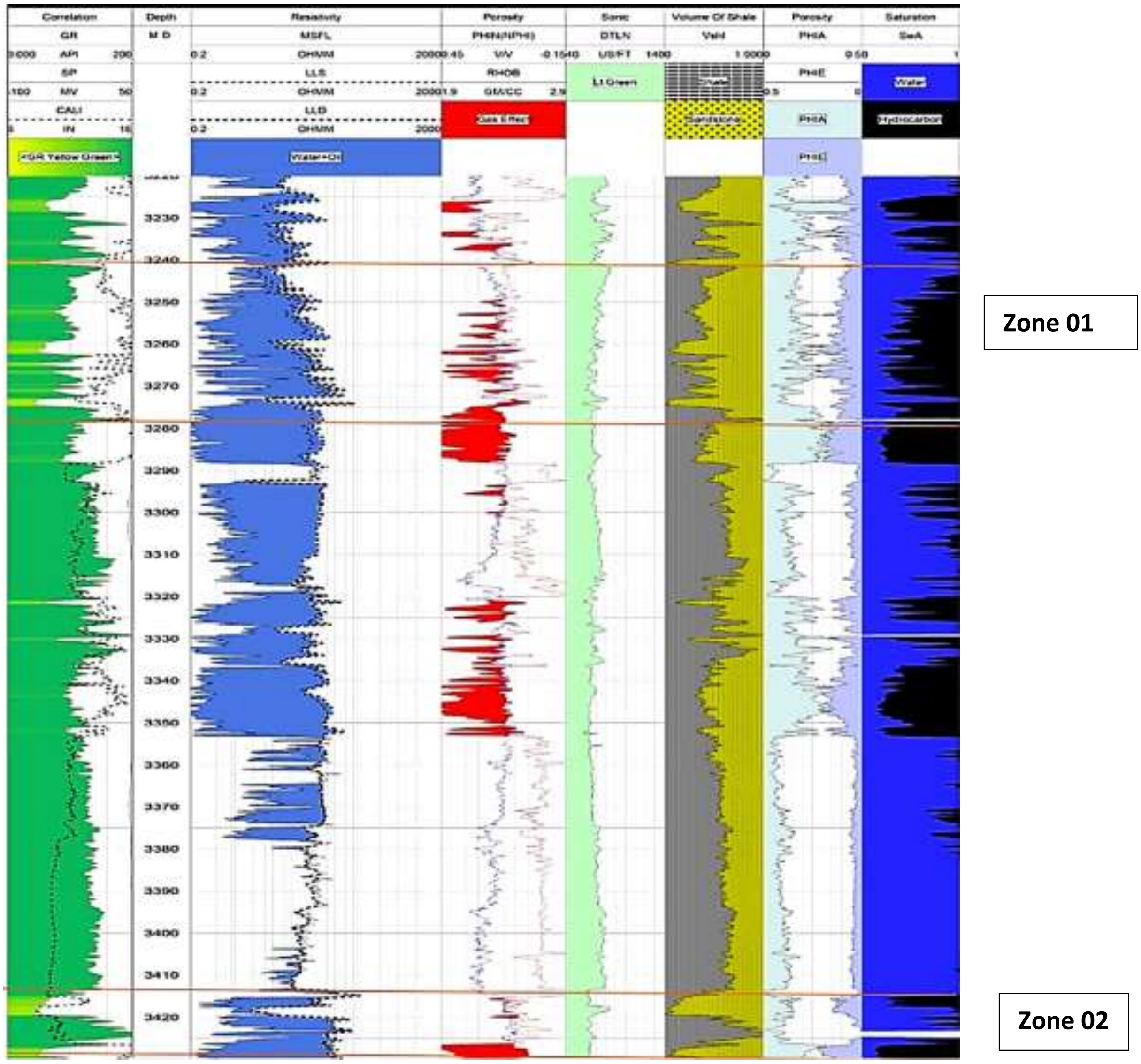

Figure 4. 5 Interpreted raw log curves of Miano 03 Well.

Table 4.4 Calculated parameters of Zone 1 (Miano 03 well)

Zone 1		
Depth	**3242-3318m**	**Average (%)**
Vsh	0.18	18
PHIA	0.28	28
PHIE	0.24	24
Swa	0.26	26
Sw	0.26	26

Table 4.5 Calculated parameters of Zone 2 (Miano 03 well)

Zone 2		
Depth	3418-3428m	**Average (%)**
Vsh	0.35	35
PHIA	0.17	17
PHIE	0.13	13
Swa	0.58	58
Sw	0.56	56

Zone 1 is identified as a possible hydrocarbon-bearing reservoir based on the combined response of various petrophysical data. The caliper log is stable, indicating acceptable borehole conditions and accurate log measurements. The gamma ray log displays low values near the sand baseline, indicating a clean sandstone formation with low shale concentration.

The resistivity logs show high deep resistivity with a distinct difference between shallow and deep curves, indicating hydrocarbon saturation within the uninvaded zone. The neutron-density logs provide a clear crossover effect, indicating the presence of gas hydrocarbons. Furthermore, the sonic log shows raised DT values, indicating increased porosity and lower acoustic velocity.

The combined log replies demonstrate that Zone 1 is a clean, porous, hydrocarbon-bearing reservoir interval with high reservoir quality.

Zone 2 is identified as a secondary hydrocarbon-bearing region using integrated well log analysis. The caliper log is relatively stable, indicating good drilling conditions and trustworthy data collecting. The gamma ray log has relatively low values, indicating cleaner lithology with less shale material.

The resistivity logs show moderately high deep resistivity values, with some divergence between the shallow and deep resistivity curves, indicating potential hydrocarbon saturation. The neutron-density logs show modest crossover behavior, confirming the presence of hydrocarbons, but weaker than in Zone 1.

The sonic log also shows unusually high DT values, indicating the presence of porosity in the formation. Overall, the results show that Zone 2 is a thinner and weaker, but potentially hydrocarbon-bearing reservoir interval.

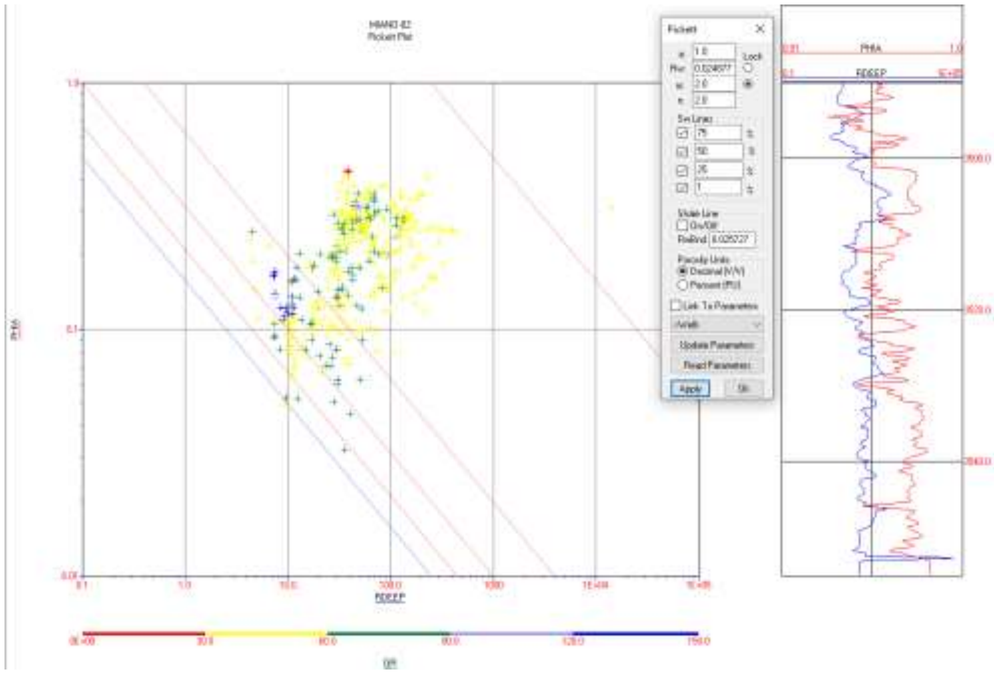

Figure 4. 6 Pickett plot of Miano 02Well in Lower Goru Formation

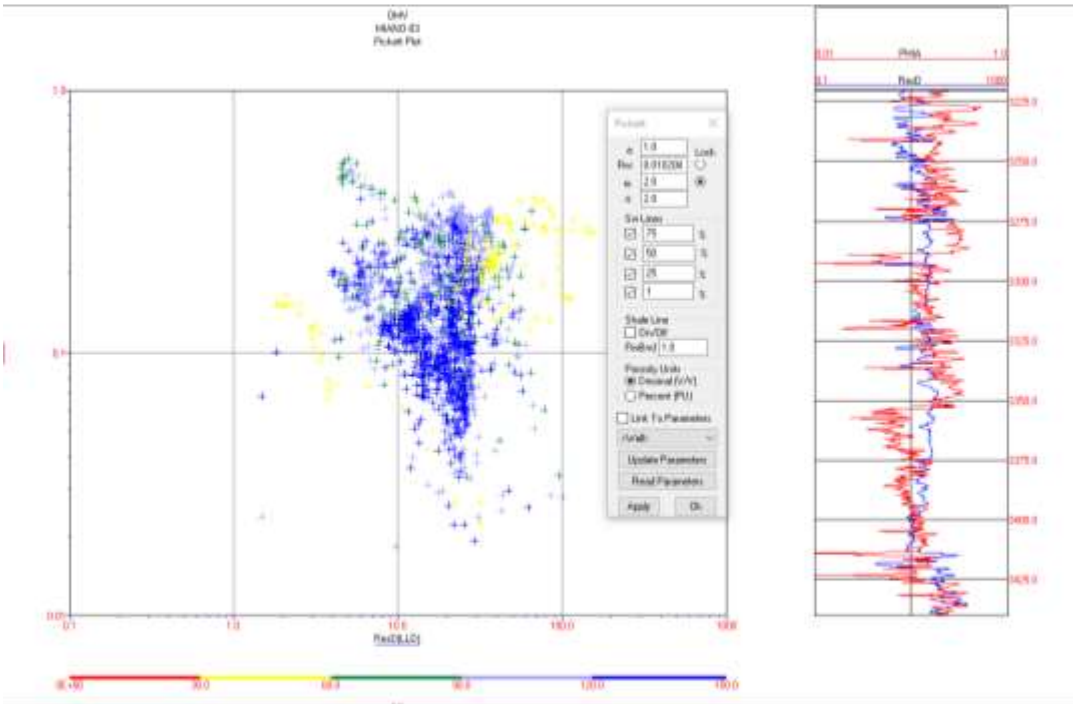

Figure 4. 7 Pickett plot of Miano 03Well in Lower Goru Formation

4.6.1 Interpreted log well 02 & 03

The raw log analysis of Miano-02 Well indicates that Zone 1 (3495–3558 m) is a relatively clean sandstone reservoir with a low shale volume (Vsh) of 12%. The average total porosity (PHIA) and effective porosity (PHIE) are 27% and 24%, respectively, indicating good reservoir quality and storage capacity. However, the water saturation values (Swa = 92% and Sw = 80%) are very high, suggesting that the zone is predominantly water-bearing with limited hydrocarbon accumulation despite its favorable porosity characteristics.

The raw log interpretation of Miano-03 Well shows that Zone 1 (3242–3318 m) is a clean reservoir interval with a shale volume of only 18%. The zone exhibits excellent reservoir properties, with average total porosity (PHIA) of 28% and effective porosity (PHIE) of 24%. The low water saturation value (Sw = 26%) indicates significant hydrocarbon saturation within the pore spaces. Therefore, Zone 1 is considered a promising hydrocarbon-bearing reservoir with good storage and production potential.

Zone 2 of Miano-03 Well, located between 3418 and 3428 m, shows poorer reservoir characteristics compared to Zone 1. The shale volume increases to 35%, indicating a shalier interval. Total porosity (PHIA) and effective porosity (PHIE) decrease to 17% and 13%, respectively, reflecting reduced pore space. Additionally, the water saturation values (Swa = 58% and Sw = 56%) are relatively high, suggesting limited hydrocarbon presence. Overall, Zone 2 represents a lower-quality reservoir with less favorable hydrocarbon potential.

CONCLUSION

An integrated seismic and well-based study to assess the Lower Goru Formation in the Miano study region, as well as the Sui Main Limestone and Ranikot formations.

A significant reservoir in this area is the Lower Goru Formation, which can produce more when more sophisticated methods are used.

Based on the analysis of seismic data, we found that the Miano region is dominated by normal faults with minor throw, suggesting the presence of extensional tectonics. However, by looking at these faults, it is possible to determine that the area possesses graben and horst structures that aid in the buildup of hydrocarbons.

Four horizons—the Upper and Lower Goru Formation of the Cretaceous age, Sui Main Limestone of the Eocene age, and the Ranikot of the Paleocene age have been identified on seismic lines in the thesis. To further corroborate the structure seen on the seismic section, time and depth contour maps have been created for these horizons.

The Miano 02 and Miano-03 wells use Lower Goru as a reservoir. In Miano 02 and Miano-03 wells, respectively, two target reservoir zones have been identified. Zone 1 of the Minao 02 well and Zone 1 and Zone 2 of the Miano 03 well have the shale volume and the hydrocarbon concentration potential.

REFERENCES

Ahmed, R., All, S. M., & Ahmad, J. J. P. J. o. H. R. (1994). Review of petroleum occurrence and prospects of Pakistan with special reference to adjoining basins of India, Afghanistan and Iran. 6(1 & 2), 7-18.

Bakker, P. (2002). Image structure analysis for seismic interpretation: Citeseer.

Jadoon, Saif Ur Rehman & Mehmood, Muhammad & Shafiq, Zohaib & Jadoon, Ishtiaq. (2016). Structural Styles and Petroleum Potential of Miano Block, Central Indus Basin, Pakistan. International Journal of Geosciences. 07. 1145-1155.

N. Khan, A. Konaté and P. Zhu, "Integrated Geophysical Study of the Lower Indus Platform Basin Area of Pakistan," International Journal of Geosciences, Vol. 4 No. 9, 2013

Khan, N. Integrated Geophysical Study of the Lower Indus Platform Basin Area of Pakistan.

Islam, G. A., Nipa, F. Y., & Shah, M. S. J. I. J. o. A. G. (2017). Petro physical properties

Herron, D. A. (2011). First steps in seismic interpretation: Society of Exploration Geophysicists.

Serra, O. (1984). The acquisition of logging data: Part A: Elsevier.

Sheriff, R. E. (2012). Seismic stratigraphy: Springer Science & Business Media.

Sheriff, R. E., & Geldart, L. P. (1995). Exploration seismology: Cambridge university press.

Kazmi, A. H., and Jan, M, Q 1997. Geology and tectonic of Pakistan petroleum Ltd, Karachi, Pakistan:Pakistan Petroleum Ltd., p.275.

Raza H.A., Ali. S.M., Ahmed, R. and Ahmed, J., 1989. Petroleum prospects: Sulaiman sub-basin, Pakistan. Pakistan Journal of Hydrocarbon Research, v.1, no.2, 21-56.

Manawar Pervaiz, Yanfei Wang, Muhammad Toqeer, Petrophysical and seismic inversion analysis for reservoir characterization of the B-interval, Lower Goru Formation, Miano Area, Central Indus Basin, Pakistan, *Journal of Geophysics and Engineering*, Volume 23, Issue 1, February 2026, Pages 1–20,

Tiab, D., & Donaldson, E. C. (2024). Petrophysics: theory and practice of measuring reservoir rock and fluid transport properties: Elsevier.

18% Overall Similarity

The combined total of all matches, including overlapping sources, for each database.

Match Groups

160 Not Cited or Quoted 17%

Matches with neither in-text citation nor quotation marks

6 Missing Quotations 1%

Matches that are still very similar to source material

0 Missing Citation 0%

Matches that have quotation marks, but no in-text citation

0 Cited and Quoted 0%

Matches with in-text citation present, but no quotation marks

Top Sources

3%	Internet sources
6%	Publications
16%	Submitted works (Student Papers)